1987

Sedimentology of the Sundance Formation, northern Wyoming

David Mason Uhlir
Iowa State University

8716832

Uhlir, David Mason

SEDIMENTOLOGY OF THE SUNDANCE FORMATION, NORTHERN WYOMING

Iowa State University PH.D. 1987

University
Microfilms
International 300 N. Zeeb Road, Ann Arbor, MI 48106

Sedimentology of the Sundance Formation,

northern Wyoming

by

David Mason Uhlir

A Dissertation Submitted to the

Graduate Faculty in Partial Fulfillment of the

Requirements for the Degree of

DOCTOR OF PHILOSOPHY

Department: Earth Sciences
Major: Geology

Approved:

Signature was redacted for privacy.

In Charge of Major Work

Signature was redacted for privacy.

For the Major Department

Signature was redacted for privacy.

For the Graduate College

Iowa State University
Ames, Iowa

1987

TABLE OF CONTENTS

Page

LIST OF FIGURES

CHAPTER I. INTRODUCTION

Study Area

The majority of the data presented and interpreted in this dissertation was collected at outcrops of the Upper Jurassic Sundance Formation in northern Wyoming. In northern Wyoming, the Sundance Formation is exposed on the margins of the Bighorn, Powder River, and Wind River Basins (Figure 1). The Sundance Formation also is exposed in more central parts of these basins where the younger rocks have been eroded above major anticlinal and domal structures.

The most concentrated field study was accomplished in north-central Wyoming (43°N-45°N latitude, 106°W-109°W longitude) which includes the southwestern margin of the Powder River Basin, the northern Wind River Basin and the Wyoming portion of the Bighorn Basin. In addition to the locations of stratigraphic sections listed in APPENDIX A, observations pertinent to this research were made at outcrops on the perimeter of the Black Hills of western South Dakota and eastern Wyoming, and along the western flanks of the Pryor Mountains of south-central Montana.

Research Objectives

The primary goal of this research was to develop paleo-environmental and paleogeographic models for the deposition of the Sundance Formation in northern Wyoming. These models should define the processes responsible for the transport, deposition

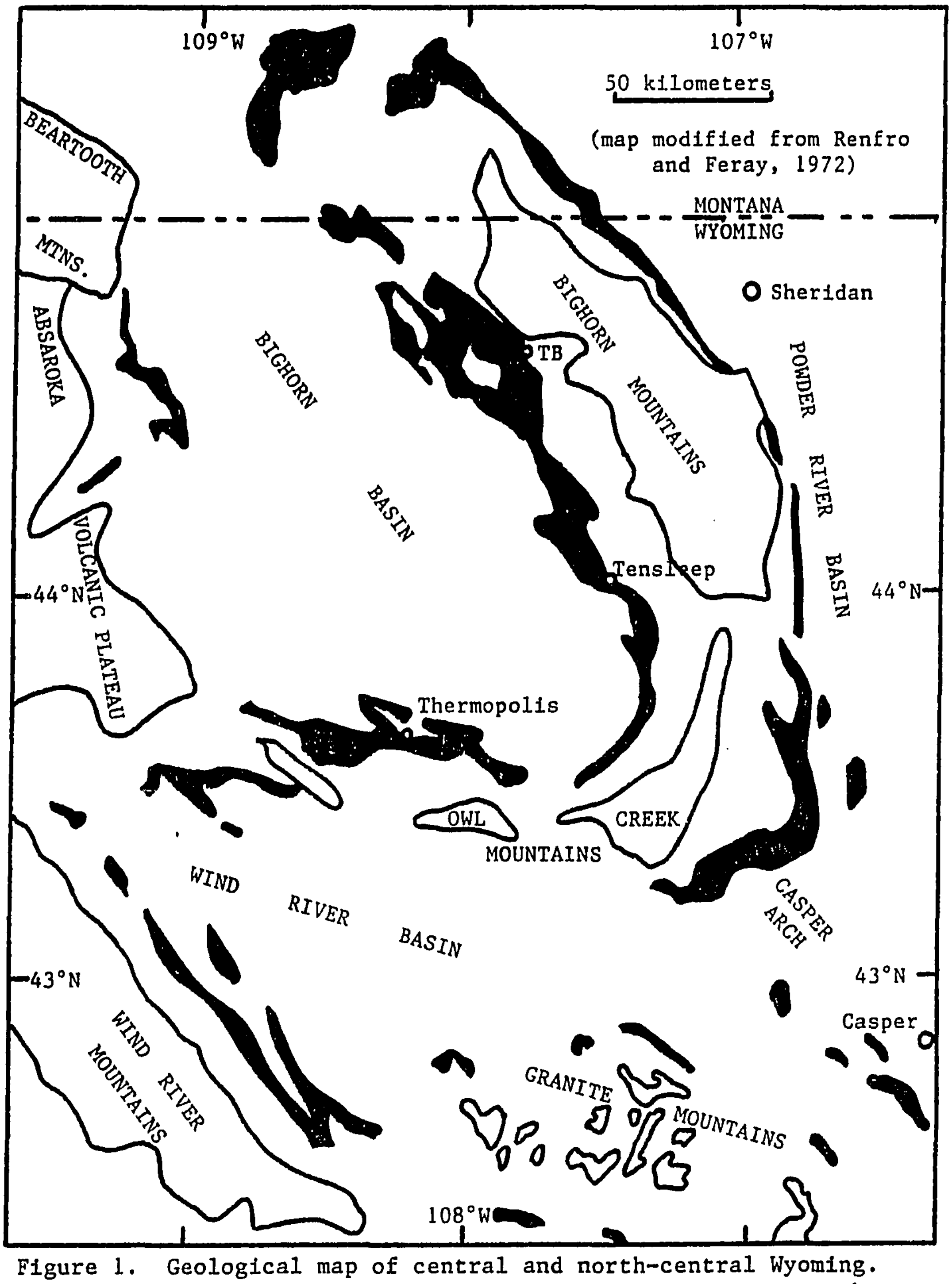

Figure 1. Geological map of central and north-central Wyoming. Upper Jurassic and Lower Cretaceous outcrops are shown in black, TB denotes tidal bundle locality

and preservation of the various lithofacies of the Sundance Formation. They should also offer explanations for regional variations in the thickness, lithology and sedimentary structures observed within each lithofacies.

Before the initiation of this research, cyclic cross-stratification patterns called "tidal bundles" had been noted in sandstones of the upper part of the Sundance Formation. A detailed description of these tidal bundles is included in the DEPOSITIONAL ENVIRONMENT chapter of this dissertation. One of the reasons for establishing models for the deposition of the Sundance Formation was to place the tidal bundles within a paleo-environmental context.

Another goal of this research was to refine the paleo-environmental and paleogeographic interpretations made by other workers. Most of these previous studies were of a more regional nature than the present study. Restricting the areal and stratigraphic scope of this study to northern Wyoming allowed observations to be made on a much smaller scale than was feasible in the more regional investigations. The increased detail of this study promised to lend greater resolution to the general conclusions made in the previous work.

Study Methods

Four field seasons were spent studying the Sundance Formation at outcrops in northern Wyoming. This fieldwork forms the bulk of the research for this dissertation. The data collected in the field consist of measured stratigraphic sections, paleocurrent measurements, and descriptions of primary hydrodynamic and biogenic sedimentary structures. Still photography was used to document these observations.

Stratigraphic sections

Outcrops were measured using a 1.5 m staff with decimeter and centimeter graduations. Where warranted by the nature of the outcrop, a pocket transit was employed in conjunction with the staff to ensure that the true thickness of the strata was measured. Sedimentation units were established on the basis of variations in lithology and sedimentary structure assemblages. The thickness of each of unit was noted, along with its lithology, overall geometry (e.g., tabular, lenticular, etc.) sedimentary structures and contact relations. All samples collected during the measurement of the outcrops were labelled with the locality name, the unit from which the sample was collected, a geopetal notation and, in some cases, the unit's strike and dip.

Sedimentary structures

The type, scale, geometries and interrelationships of the sedimentary structures were noted, sketched and photographed during the measurement of the stratigraphic sections. The types of bedforms active during the deposition of each unit were deduced from the scale and geometry of the stratification and cross-stratification. These interpretations were made with as much detail as is afforded by the exposures (e.g., differentiating sinuous-crested current ripples from straight-crested forms). The stratification set thicknesses were measured. When practical, the wavelengths, amplitudes, foreset inclinations and climb angles of cross-stratification sets were noted. Stratification sets were inspected for evidence of truncation, biogenic disturbance and soft-sediment deformation. Within sandstone units, mud drapes and other fine-grained films were described in terms of thickness, lateral continuity, stratigraphic position and association with the stratification (e.g., "2 mm-thick, laterally continuous mud drapes overlie the current ripple cross-lamination in the upper third of this unit"). The occurrence and degree of development of erosion surfaces within the strata were described. The degree of incision of erosion surfaces was described in terms of relief over lateral distance (e.g., "0.5 m relief in 10 m").

Paleocurrent measurements

Wherever possible, the paleocurrent directions recorded within the primary structures of a unit were measured. The compass of the pocket transit was used for these measurements. In areas with extensive bedding-plane exposures of a single unit, many paleocurrent measurements were taken along traverses. Each paleocurrent measurement is paired with a notation about the type and scale of sedimentary structure from which it was derived. Certain bedforms (e.g., parting lineation) may be interpreted to have been formed from a current flowing in one of two directions. These two possible paleocurrent directions are in 180° opposition to one another. In these cases, both possible directions were recorded as a couplet separated by a slash (e.g., 090/270). A stereonet was used to correct the paleocurrent directions measured at outcrops where the strata are inclined more than 15°. Corrections were not made to measurements taken at outcrops dipping at less than 15° because the influence of the outcrop inclination is within the limits of precision (± 1°, approximately) of the measurements.

Laboratory methods

Petrological investigations Several methods of laboratory analysis were used to study samples collected during the fieldwork. To verify and calibrate the grain-size estimates made in the field, dry-sieve grain size analyses were carried out on selected sandstone samples. Loose-grain mounts were prepared from the 2-4 phi (fine- to very fine-grained sand), the medium-grained sand and coarser (less than 2 phi), and the coarse to medium silt (4-6 phi) size fractions. The loose-grain mounts were inspected using a binocular, fixed-stage microscope. The mineralogy of the clay-sized fraction was analyzed by X-ray diffraction. Petrographic thin-sections were inspected using a polarizing microscope.

Paleohydrodynamic modelling

The paleotidal range of the environment in which the tidal bundles were formed was estimated through the use of numerical sediment transport models. The geometry (set thickness and coset height) of the bundled cross-stratification was controlled by the velocity of paleotidal currents. The tidal current velocity in a particular location is proportional to the tidal range at that location. Using this rationale, the paleotidal range of the tidal bundle-forming environment was estimated from the geometry of the cross-stratification of the tidal bundles.

CHAPTER II. PREVIOUS WORK

Preface

The bulk of this dissertation concerns sedimentological interpretations based on observations made in the upper part of the Sundance Formation. In the interest of placing these sedimentological interpretations within a stratigraphic framework, this chapter concentrates on the previous work which establishes the stratigraphic nomenclature and correlation of this interval, and its general depositional setting.

History of Stratigraphic Nomenclature

In 1857, Meek and Hayden described a series of gray marls with intercalations of calcareous sandstone outcropping around the margin of the Black Hills of western South Dakota and eastern Wyoming. From abundant, well-preserved fossils present in these marls, Meek and Hayden assigned them to the Jurassic. Knight (1900) described marine Jurassic units in southeastern Wyoming and called them the "Shirley Stage."

In 1904, Darton (p. 387) named the "marine Jurassic sediments of the Black Hills region" the Sundance Formation. The name "Sundance" was derived from that of "the town in the northern part of the [Black Hills] uplift." Darton (1904, p. 398) lithologically correlated outcrops of "Typical marine Jurassic deposits..." on the margins of the Bighorn Mountains with the Sundance Formation, stating that "They are so similar to the deposits in the Black Hills that the same name is applicable."

In a primarily paleontological work, Crickmay (1936) divided the marine Jurassic deposits of central and eastern Wyoming into three separate units, the Lower, Middle and Upper Sundance formations. Crickmay's (1936) correlation of the Lower Sundance Formation was based upon its lithologic similarity within his study area. The presence of the belemnite Pachyteuthis densus defined his Middle Sundance Formation. His Upper Sundance consisted of the strata above the belemnite zone and below the base of the Morrison Formation. Crickmay's (1936) division of the Sundance Formation has not been formally adopted.

Cobban (1945) named the Swift Formation from exposures near Swift Reservoir on Birch Creek in northwestern Montana. Using the age determinations of R.W. Imlay, Cobban (1945) assigned the Swift Formation to the Argovian and upper Divesian substages of the Oxfordian. Imlay (1947) proposed the "Redwater Shale Member" as the name for the Oxfordian strata of the upper part of the Sundance Formation. The type section of the Redwater Shale Member of the Sundance Formation is in western South Dakota, near the town of Spearfish. Imlay (1947, p. 227) correlated the Redwater Shale Member "with highly glauconitic sandstone and shale farther west, variously called the Swift Formation, Stump Sandstone, Curtis Formation and 'Upper Sundance' Formation."

The term "Upper Sundance" Formation is an informal designation, first cited by Neely (1937). The term was used primarily within the petroleum industry. Peterson (1954) proposed raising the unit to full formational status. His evidence showed that the "Lower Sundance" Formation and the "Upper Sundance" Formation each represented the deposits of "a single cycle of transgression and regression during separate stages [Callovian and Oxfordian respectively] of [Late] Jurassic time" (Peterson, 1954, p. 473). Peterson (1954) correlated the "Lower Sundance" and "Upper Sundance" formations of Wyoming with the Rierdon and Swift formations (respectively) of Montana. Peterson's (1954) proposal was not accepted by later workers. Imlay (1956) and Love (1958) referred to the "lower" and "upper" Sundance formations, implying they regarded the division of the Sundance Formation as informal.

From outcrops on the eastern and southern margins of the Bighorn Basin, Imlay (1956) divided the "upper" Sundance Formation into an upper and lower member. The lower member consists "mostly of soft, fissile, medium gray calcareous claystone interbedded with some silty to sandy chunky glauconitic claystone" (Imlay, 1956, p. 596). The upper member consists of calcareous and glauconitic sandstone, typically containing "one or more beds of sandy coquina 1-12 feet [0.3-3.7 m] thick" (Imlay, 1956, p. 596). On the basis of this description, the writer concludes that the upper sandstone member of the "upper" Sundance Formation (sensu Imlay, 1956) comprises the "sandstone facies" and "coquina facies" described in the DEPOSITIONAL ENVIRONMENT chapter of this dissertation.

From sections measured in south-central Wyoming, Pipiringos (1968) divided the Sundance Formation into seven members. From lowest to highest these were: the Canyon Springs Sandstone, the Stockade Beaver Shale, the Hulett Sandstone, the Lak Member, the Pine Butte Member, the Redwater Shale and the Windy Hill Sandstone. The stratigraphic relations of the seven members of the Sundance Formation are summarized in Figure 2.

Pipiringos and O'Sullivan (1978, p. A26) stated that "The uppermost dated beds of the Redwater Shale Member are of middle Oxfordian age..." in eastern and central Wyoming. From its interfingering relationship with the lowermost Morrison Formation, Pipiringos and O'Sullivan (1978) considered the Windy Hill Sandstone Member to be of probable Kimmeridgian age.

Paleogeographic and Paleotectonic Setting

The Sundance Formation was deposited within and on the margins of two successive epicontinental seaways. The earlier sea occupied the western interior of North America in the late Middle Jurassic (early to middle Callovian). The lower part of the Sundance Formation (Canyon Springs Sandstone Member through Lak Member) was deposited in this Callovian sea. The Redwater

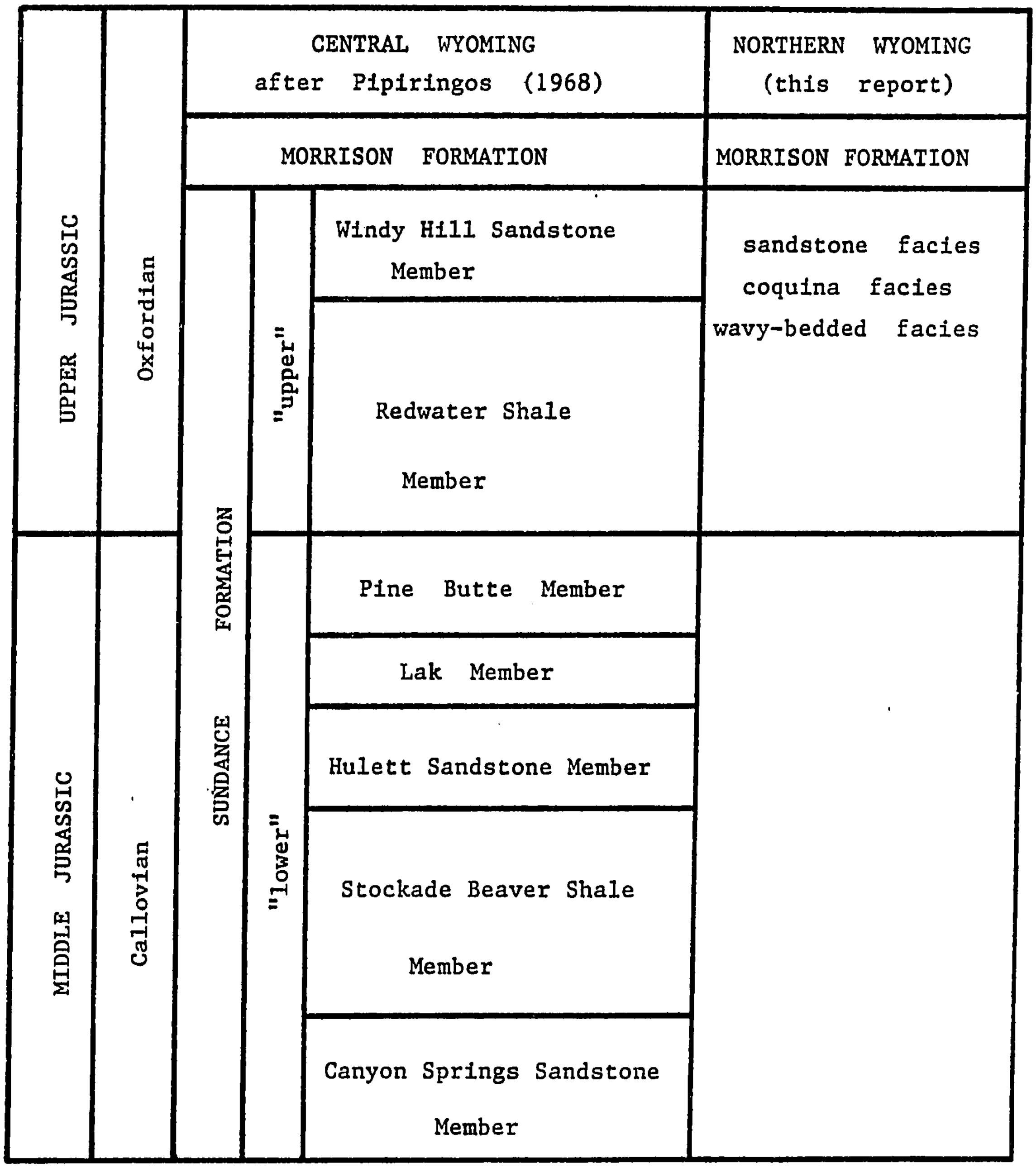

Figure 2. Diagram illustrating the stratigraphic relationship of the formal and informal subdivisions of the Sundance Formation and their probable correlation with the facies described in this report

Shale Member was deposited in the later (early to middle Oxfordian) seaway (Imlay, 1952, 1980). The Windy Hill Sandstone Member may be the result of a minor, still later cycle of transgression and regression (Imlay, 1980).

During periods of maximum transgression, both of these seaways had a roughly lingoid shape with their northern parts connecting to the open marine waters of the Arctic Ocean (Imlay, 1952). These lingoid seaways were situated inland of the subduction zone and volcanic arc then active along the western margin of North America (Dickinson, 1976, 1981). The plutonism and horizontal compression associated with this orogeny may have been the impetus for deep crustal shortening and shallow thrusting in between the (Sierra Nevada) volcanic arc and the western margins of the Sundance seaways (Allmendinger and Jordan, 1981).

The parallelism of the long axes of the lingoid seaways with the trend of the tectonic belt to the west may be the result of more than coincidence. The epicontinental seaways in which the Sundance Formation was deposited may have been foreland basins caused, at least in part, by the crustal loading associated with the Nevadan orogeny. Unlike some of the Late Cretaceous seaways (marine foreland basins of the Sevier orogeny) the Middle and Late Jurassic seaways never connected the Arctic Ocean with the Gulf of Mexico (Swain and Peterson, 1951; Imlay, 1952).

The Oxfordian transgression created the most extensive of the Jurassic seaways (Figure 3). At its maximum, marine waters covered most of Alberta, Montana, Wyoming, northern Colorado, eastern Utah, southern Saskatchewan, western North Dakota, western South Dakota and western Nebraska (Imlay, 1952, 1980; Peterson, 1972; Brenner, 1983;). The Alberta trough, the deepest part of the seaway in Canada, was immediately adjacent to the active thrust front of the Columbian (Nevadan phase) orogen (Poulton, 1984). In the United States, the early Oxfordian transgression progressed southward into Montana, Wyoming and Colorado. During this southerly elongation, the seaway widened, transgressing towards the east into the Dakotas and west into Utah (Imlay, 1980).

The coarse-grained sediments (sand-size and larger, excepting bioclasts) of the upper part of the Sundance Formation may have been derived from highlands to the west of the Oxfordian seaway (Brenner and Davies, 1973, 1974; Imlay, 1980) from "a persistently rising area in south-central Colorado" (Imlay, 1980, p. 108) and from a number of areas of emergence within the seaway itself. The following section discusses some of the evidence which supports the existence of these emergent areas, or islands, within the Oxfordian seaway.

<u>Local unconformities</u>

Moritz (1951, p. 1805) attributed the lack of marine Middle

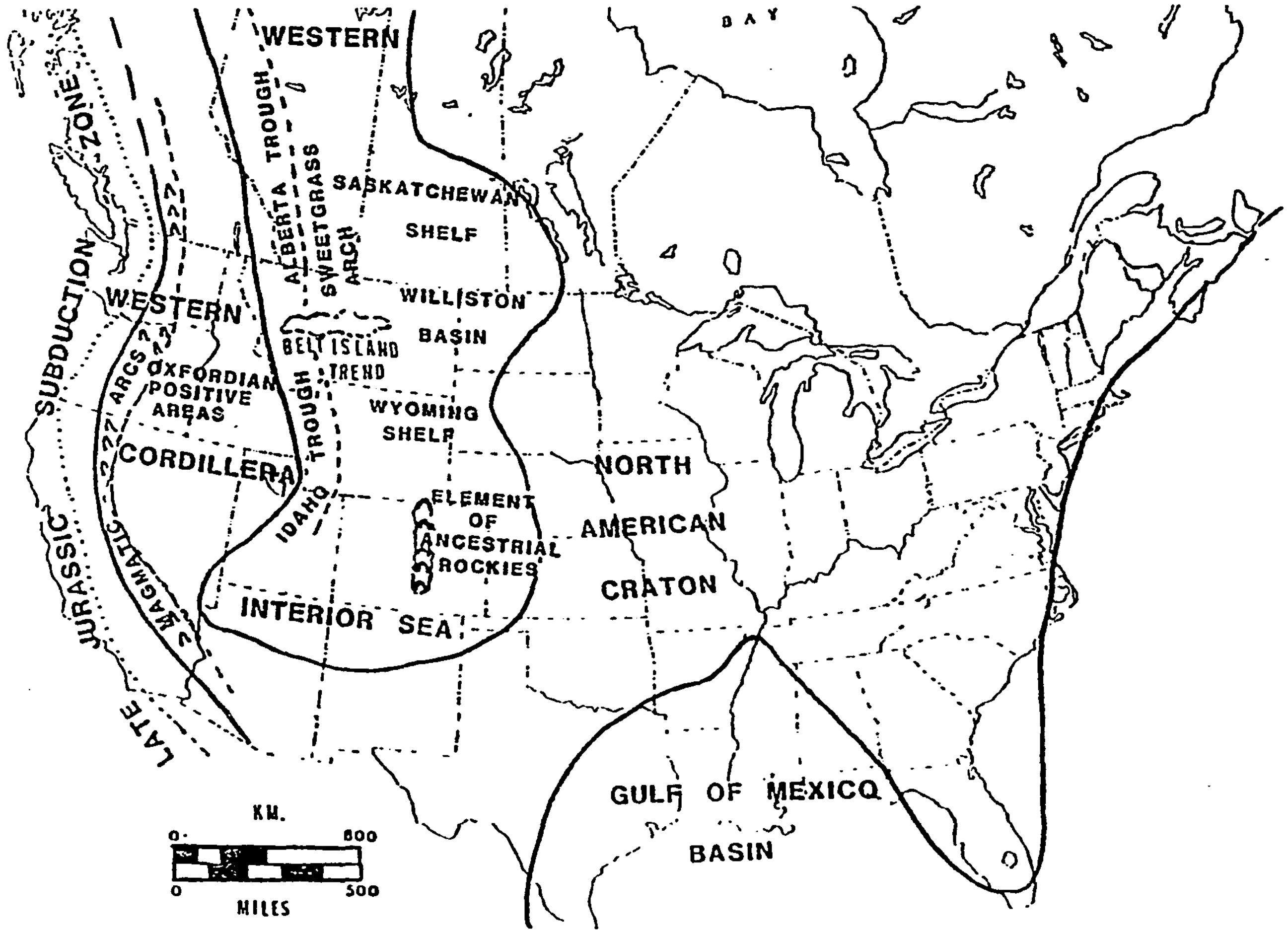

Figure 3. Map of the paleogeography and major tectonic elements of North America during Oxfordian time (from Brenner, 1983)

and Upper Jurassic rocks (Piper, Rierdon and Swift formations) in a portion of southwestern Montana to the presence of a "small, but prominent positive area..." during the time of their deposition. The formations of the Ellis Group thicken uniformly in all directions away from this protuberance. Imlay's (1947) "Belt Island" and the "Belt Island Trend" of Brenner and Davies (1974) correspond to this Middle and Late Jurassic positive structural element (Figure 3). Brenner and Davies (1974) cited local zones of chert pebble conglomerate in the Swift Formation's transgressive units as evidence for the uplift. The conglomerates lack the heavy minerals that would be indicative of derivation from igneous or metamorphic rocks, so Brenner and Davies (1974) concluded that they are of sedimentary, upper Paleozoic provenance. Brenner and Davies (1974) did not find similar conglomerates in the upper part of the Sundance Formation in Wyoming, so they concluded that the effects of the uplift were confined to Montana.

Imlay (1956, p. 598) explained thinning of the "upper" Sundance Formation near Tensleep, Wyoming (Figure 1) as probably reflective of "local uplift during Sundance time." The presence of similar Late Jurassic positive elements is suggested by the areal distributions of chert clasts in the uppermost Sundance Formation of north-central Wyoming (Uhlir, 1987) and of eolian sandstones in the lower Morrison Formation of central Wyoming

(Uhlir, 1986; Weed and Vondra, 1987). The TECTONIC IMPLICATIONS chapter of this dissertation includes a more thorough discussion of the significance of these clastic chert and eolian sandstone distributions.

J-5 unconformity and the Windy Hill Sandstone Member

Rather than viewing the local truncation of the Sundance Formation as the expression of discrete areas of emergence during Sundance deposition, Pipiringos and O'Sullivan (1978) believed an episode of general erosion occurred in the western interior during late Oxfordian time. Pipiringos and O'Sullivan (1978) referred to the erosional surface developed at this time as the "J-5 unconformity." The J-5 unconformity was described as "a nearly flat even surface; a surface almost unmarked by channels even where it bevels underlying units" (Pipiringos and O'Sullivan, 1978, p. A25). Where the Windy Hill Sandstone Member of the Sundance Formation is present, it overlies the J-5 unconformity. Where the Windy Hill Sandstone Member is not present, Pipiringos and O'Sullivan (1978) placed the unconformity at the base of the Morrison Formation.

The regional extents of the J-5 unconformity and of the Windy Hill Sandstone Member remain controversial. The sea in which the Redwater Shale Member of the Sundance Formation was deposited began regressing during the middle Oxfordian (Imlay, 1980). The J-5 unconformity may have developed during this initial regression. This regression was interrupted by an episode of transgression, during which the Windy Hill Sandstone Member was deposited in western South Dakota, eastern and southern Wyoming, northwestern Colorado and northeastern Utah (Pipiringos and O'Sullivan, 1978; Imlay, 1980). The correlation of the Windy Hill Sandstone Member has not been extended into Montana and north-central Wyoming. Imlay (1980, p. 113) made an informal correlation by assuming that the Windy Hill Sandstone Member was "deposited at the same time as the upper part of the marine beds lying conformably below the Morrison Formation..." in Montana and north-central Wyoming.

Imprecise dating of the inception of Morrison Formation deposition may have falsely suggested that an episode of regional erosion occurred after the deposition of the Sundance Formation. Imlay (1980) believed deposition of the Morrison Formation began in the late Oxfordian in Wyoming. Earlier work (e.g., Imlay, 1947; Pipiringos, 1968; Brenner and Davies, 1973,1974; Pipiringos and O'Sullivan, 1978) placed Morrison deposition wholly within the Kimmeridgian. The J-5 unconformity was used to explain the supposed lack of upper Oxfordian sediments in the western interior (Pipiringos and O'Sullivan, 1978). Imlay's (1980) upper Oxfordian placement of the lower Morrison Formation brought the existence of the J-5 unconformity into question. Imlay's (1980) findings also suggested that the tentative assignment of a

Kimmeridgian age to the Windy Hill Sandstone Member of the Sundance Formation (Pipiringos and O'Sullivan, 1978) should be revised to upper Oxfordian.

During the course of this research, no evidence of a surface of regional erosion between the Sundance and Morrison Formations was encountered in north-central Wyoming. Evidence for the conformable nature of the Sundance-Morrison contact in north-central Wyoming is discussed in the DEPOSITIONAL ENVIRONMENT chapter of this dissertation.

CHAPTER III. DEPOSITIONAL ENVIRONMENT

Introduction

Two models have been presented concerning the depositional environments and processes responsible for the sandstone and coquinas of the uppermost 15-20 m of the Upper Jurassic Sundance Formation of north-central Wyoming (Brenner and Davies, 1973, 1974; Brenner, Swift and Gaynor, 1985). The earlier model (Brenner and Davies, 1973, 1974) employed storm-incision of offshore sand bars. The latter model invoked storm and tidal current-induced sand wave migration across inner shelf sand ridges and storm truncation of these sand ridges to produce the sequence of sandstones and coquinas of the uppermost Sundance Formation.

The writer divides the uppermost 15-20 m of the Sundance Formation into a coquina facies and a sandstone facies (Figure 4). These facies compose the "upper sandstone member" of the Oxfordian "upper Sundance" Formation as described by Imlay (1956). The "upper Sundance" Formation is the stratigraphic equivalent of the Swift Formation of adjacent south-central Montana (Imlay, 1952; Peterson, 1954). Within the Bighorn Basin of north-central Wyoming (Figure 1) the sandstone and coquina facies are conformably overlain by the lagoonal and coastal plain sediments of the Morrison Formation (Kvale and Vondra, 1985). Clasts of coal and other organic material are locally

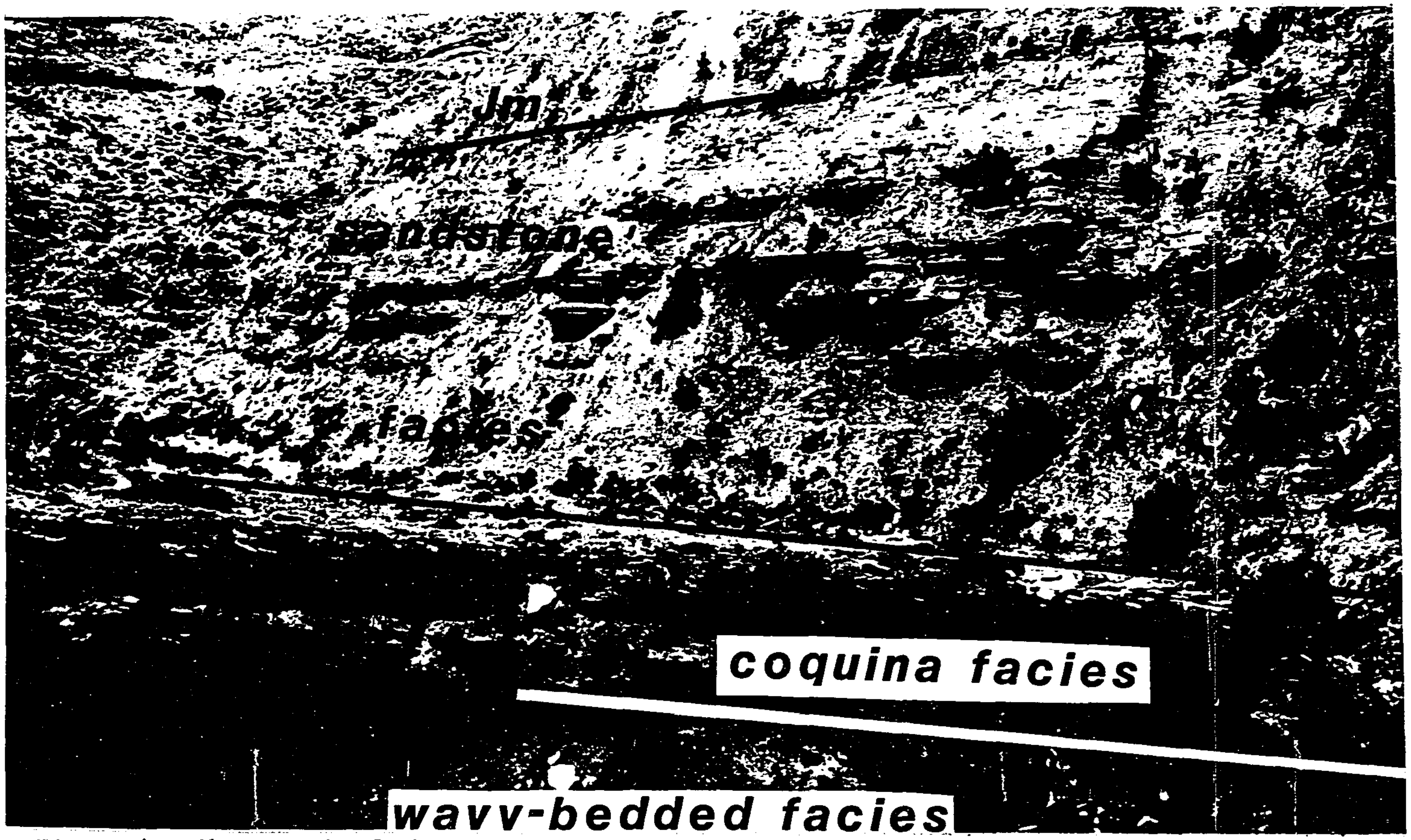

Figure 4. Photograph of the wavy-bedded, coquina and sandstone facies of the uppermost Sundance Formation, conformably overlain by the black mudstone of the basal Morrison Formation (Jm) at the LEAVITT RESERVOIR 1 locality

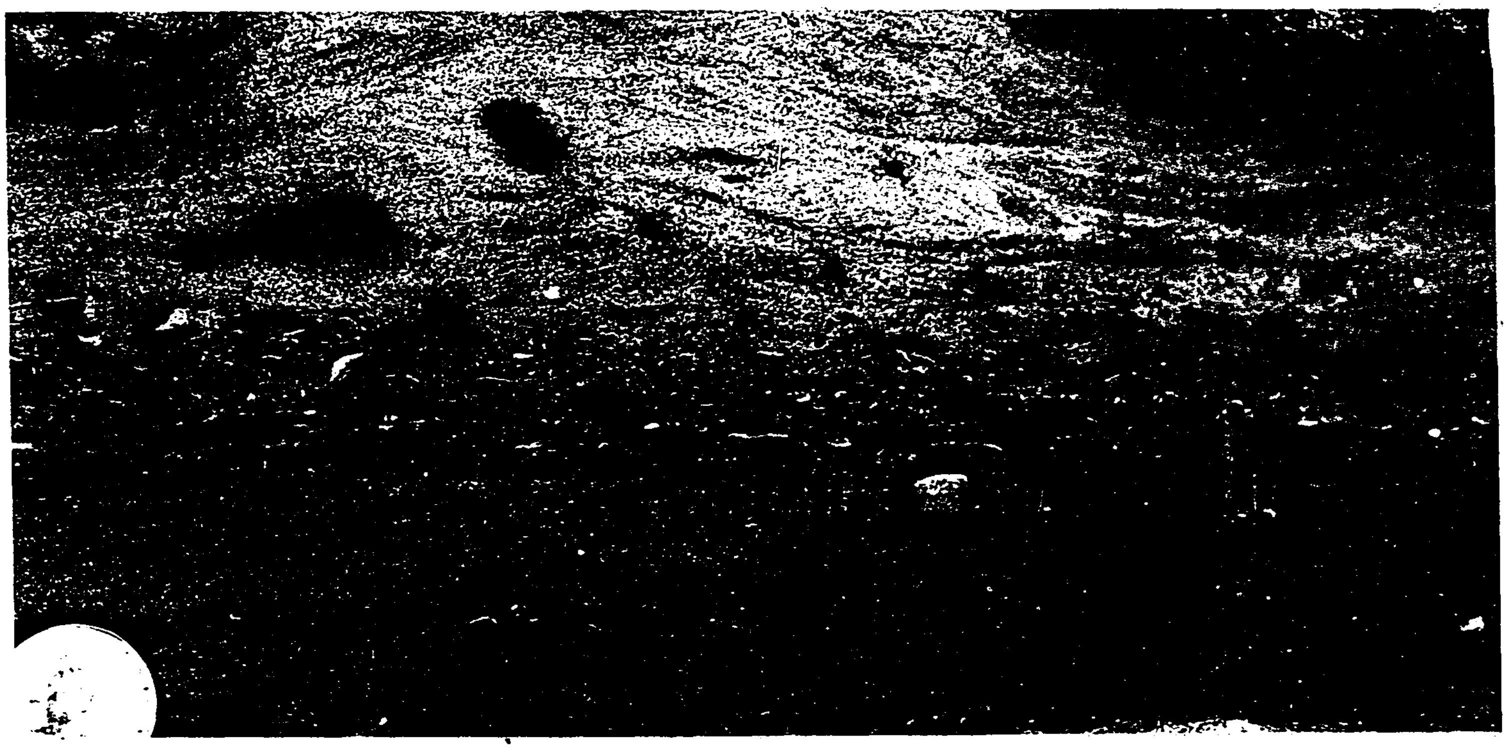

Figure 5. Photograph of coal clasts (black fragments) within the upper 2 m of the sandstone facies. Some fragmental shell material is also present. Horizontal lamination (lower 1/2 of photograph) and current ripple cross-lamination (upper 1/2 of photograph) are typical sedimentary structures in the upper part of the sandstone facies. The coin is 30 mm in diameter

incorporated into the sandstones of the uppermost Sundance Formation in the Bighorn Basin (Figure 5). The most likely source of this organic material is from the early Morrison coastal plain and marshes which fringed the late Sundance sea. The base of the coquina facies is typically erosive, having been incised into the underlying wavy-bedded facies that forms the top 15 m of the Redwater Shale Member of the Sundance Formation (Imlay, 1956; Pipiringos, 1968) a 50 m thick coarsening-upward sequence of marine claystones and siltstones.

Evidence discussed in this chapter implies that the thick horizons (up to 4 m) of the coquina facies of the uppermost Sundance Formation in north-central Wyoming were formed as the lags of tidal inlet channels migrating along a prograding, mesotidal barrier coastline. The sandstone facies represents inlet channel-fill, spit-platform, tidal delta, shoal and sandy back-barrier tidal flat deposits. Tidal bundles (Figure 6) have been described from within the sandstone facies (Elliott, 1984; Uhlir and Vondra, 1984; Uhlir, Vondra, Akers and Elliott, 1986) the details of which will be discussed later in this chapter. Thin beds (less than 0.5 m thick) of the coquina facies developed as lags of tidal creeks meandering within the back-barrier shoals and tidal flats. The subaerial deposits of this barrier coastline were prone to reworking, both from the lateral migration of the tidal inlets in response to longshore currents

Figure 6. Photograph of the exposure of 27 consecutive tidal bundles within the sandstone facies of the uppermost Sundance Formation at the SHELL 2 locality. The hammer is 0.3 m long

and from the seaward facies migration associated with the progradation of the early Morrison coastal plain environments. Thus, the subaerial barrier sequence was rarely preserved.

The uppermost Sundance Formation in north-central Wyoming was deposited in a setting dominated by tidal processes. The effects of storms are rarely discernible. The writer will discuss the stratigraphic and sedimentological evidence, modern analogues, hydrodynamics and bedform theory that suggest that a prograding, mesotidal barrier coastline was responsible for the deposition of the uppermost Sundance Formation in north-central Wyoming.

Facies Description

Sandstone facies

The sandstone facies of the uppermost Sundance Formation is composed of sublitharenites (sensu McBride, 1963) that fine upsection from fine- to very fine-grained sandstones towards the conformable contact with the organic-rich and occasionally coal-bearing basal Morrison mudstone. The sandstone facies contains from 0 to 15 percent spheroidal and lobate glauconite grains and trace amounts of sand-sized dark chert. In this report, the term glauconite is used to refer to a variety of iron- and potassium-rich hydrous aluminosilicate minerals that occur in green, sand-sized pelletal agglomerates. In this usage, glauconite is synonymous to the term glaucony proposed by Odin and Matter

(1981). The rare units in the sandstone facies that contain less than 5 percent glauconite are quartz arenites. The sandstone facies is typically friable. Calcium carbonate is the principal cement, but this cementation is generally not well developed.

Large scale (0.2 m to 0.8 m thick) trough cross-lamination sets, current ripple lamination and upper flow regime horizontal lamination are the predominant sedimentary structures of the sandstone facies. Bioturbation is rare within most of the facies, with excellent preservation of the primary sedimentary structures in all but the upper 2 m of the sandstone. Mud drapes (1 mm to 3 mm thick) are common, often overlying subordinate current ripple lamination developed on the subordinate current reactivation surfaces that truncate the large scale trough cross-lamination (Figure 7). The subordinate current reactivation surfaces are sigmoidal. They are probably the result of subordinate current modification of a large scale bedform in an asymmetrical tidal current setting. The dominant current reactivation surfaces (Figure 7) were most likely developed shortly after the reactivation of the dominant current.

The first use of the term "subordinate current reactivation surface" is by Mowbray and Visser (1984) but similar structures have been called "discontinuity planes" by Raaf and Boersma (1971), "gently inclined sigmoidal discontinuities" by Allen (1980a) and "pause planes" by Boersma and Terwindt (1981a,

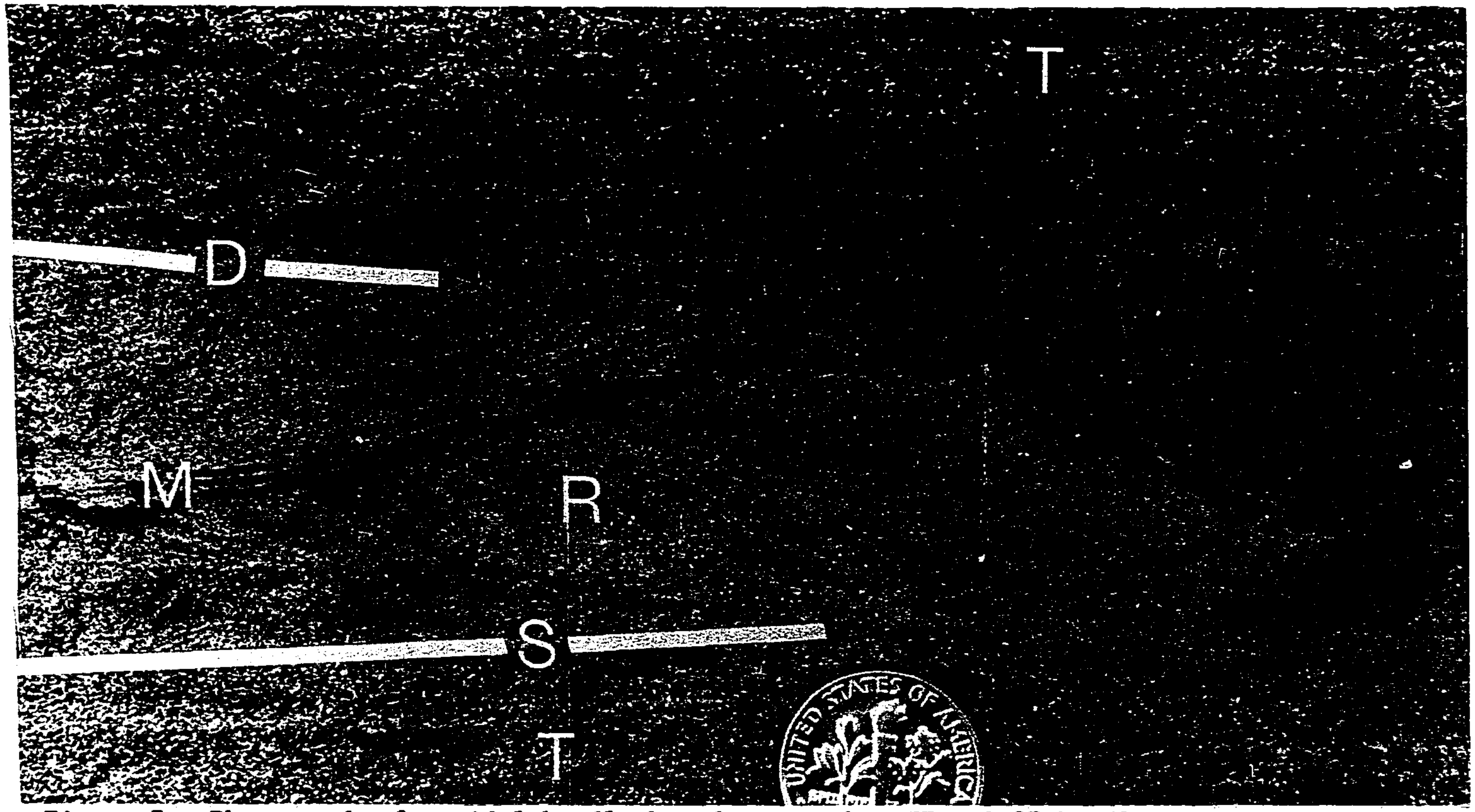

Figure 7. Photograph of a tidal bundle boundary at the SHELL 2 27-bundle exposure. Large scale trough cross-lamination (T) dipping to the left (south) is truncated by a subordinate current reactivation surface (S). The subordinate current reactivation surface is overlain by current ripple cross-lamination (R) formed by the subordinate tidal current flowing from left to right. The subordinate current ripple cross-lamination is overlain by a 2 mm thick mud drape (M). A dominant current reactivation surface (D) underlies the upper set of trough cross-lamination. The coin is 18 mm in diameter

1981b). The writer follows Mowbray and Visser (1984) in emphasizing that these subordinate current reactivation surfaces and the current ripples that often overlie them are not the result of backflow currents associated with flow separation vortices developed in the lee of the large scale bedforms. The subordinate current reactivation surfaces form the set boundaries of tidal bundles that occur within the sandstone facies (Figure 6).

Mud rip-up clasts from 1 mm to 3 mm thick are also common in the sandstone facies, lying parallel to the foresets of the large scale cross-lamination sets. These rip-up clasts are most likely derived from mud drapes subjected to "relatively strong" (Mowbray and Visser, 1984) subordinate current erosion.

It is possible, but by no means clear that the sandstone facies is equivalent to the Windy Hill Sandstone Member of the Sundance Formation (as defined by Pipiringos, 1968). Pipiringos and O'Sullivan (1978) discuss the areal distribution of the Windy Hill Sandstone Member and do not imply that it is present in north-central Wyoming. The current state of knowlwedge on this issue is discussed in the Paleogeographic and Paleotectonic Setting section of the PREVIOUS WORK chapter of this dissertation. It warrants mention that in eastern Wyoming and western South Dakota, the Windy Hill Sandstone Member of the Sundance Formation is interpreted as a transgressive shallow marine deposit (Imlay, 1980). In contrast, the sandstone facies of the uppermost Sundance Formation in north-central Wyoming (this report) appears to be a regressive shoreline deposit.

Coquina facies

The coquina facies is a biosparite (*sensu* Folk, 1959) composed primarily of *Camptonectes bellistriatus*, *Ostrea strigilecula*, and *Meleagrinella curta* fragments (Imlay, 1956) surrounding disarticulated whole valves typically resting in concave-down orientations. Fine- to medium-grained quartz sand, sand- to pebble-sized grains of black and tan chert, and pebble-sized mudstone rip-up clasts lie concentrated in varying proportions within the coquina facies (Figure 8). The internal stratification of the coquina consists of large scale (0.3 m to 1.5 m thick) sets of trough and low-angle cross-bedding (Figure 9). The low-angle cross-bedding represents lateral accretion surfaces preserved in the coquina channel lag as the tidal inlets migrated along the barrier coastline. Regular imbrication of the shell fragments can often be noted within the cross-beds.

Wavy-bedded facies

The coquina facies has an erosive base and is incised with variable amounts of relief into the thin lenses and beds of wave and current rippled very fine sandstone and intercalated mudstone laminae of the underlying wavy-bedded facies (Figure 10). The wavy-bedded facies represents the upper 15 m of the Redwater

Figure 8. Photograph of the coquina facies of the uppermost Sundance Formation. Note the rounded chert pebble in the upper center of the photograph. The coin is 24 mm in diameter

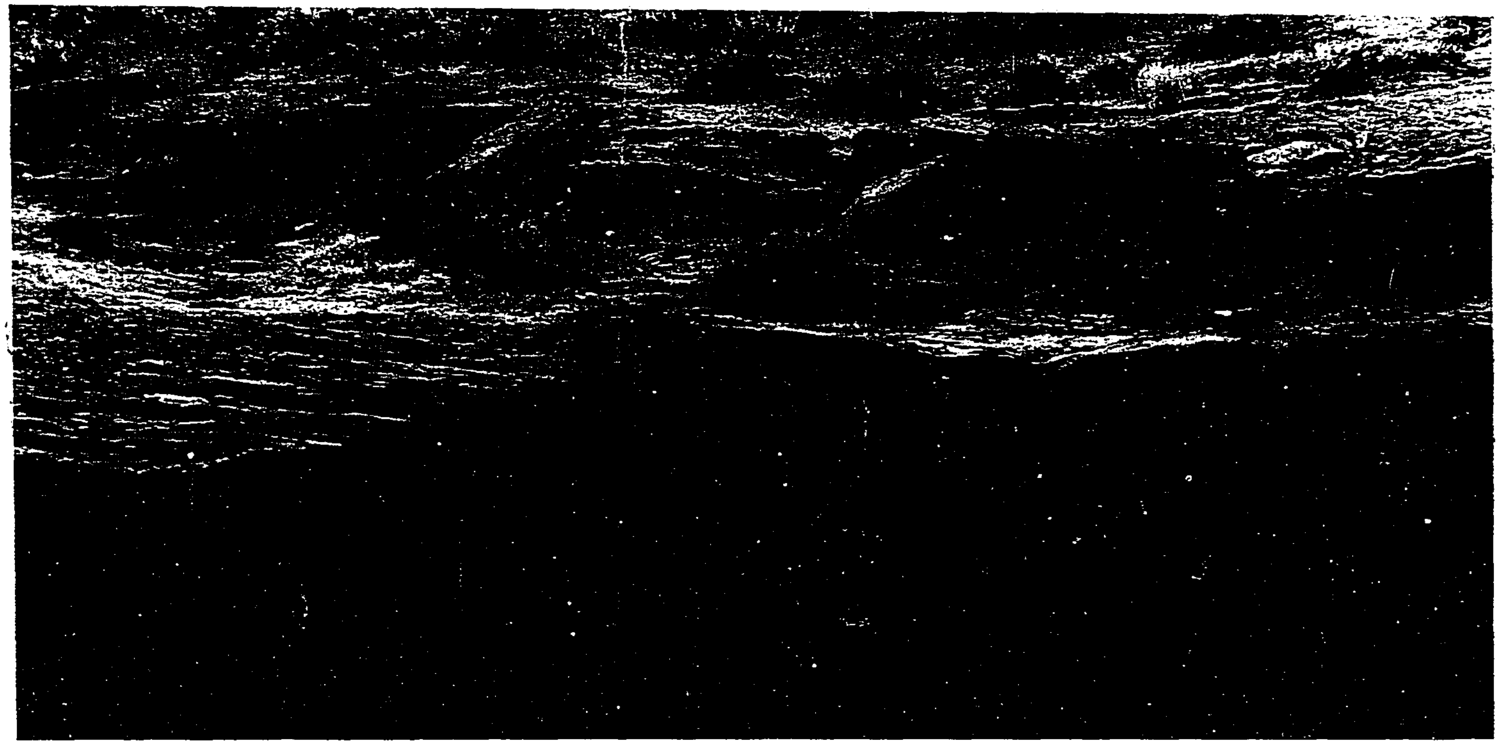

Figure 9. Photograph of erosive-based coquina facies incised into the underlying wavy-bedded facies. Lateral accretion surfaces in the coquina facies dip gently from left to right. The coquina bed is 1.1 m thick

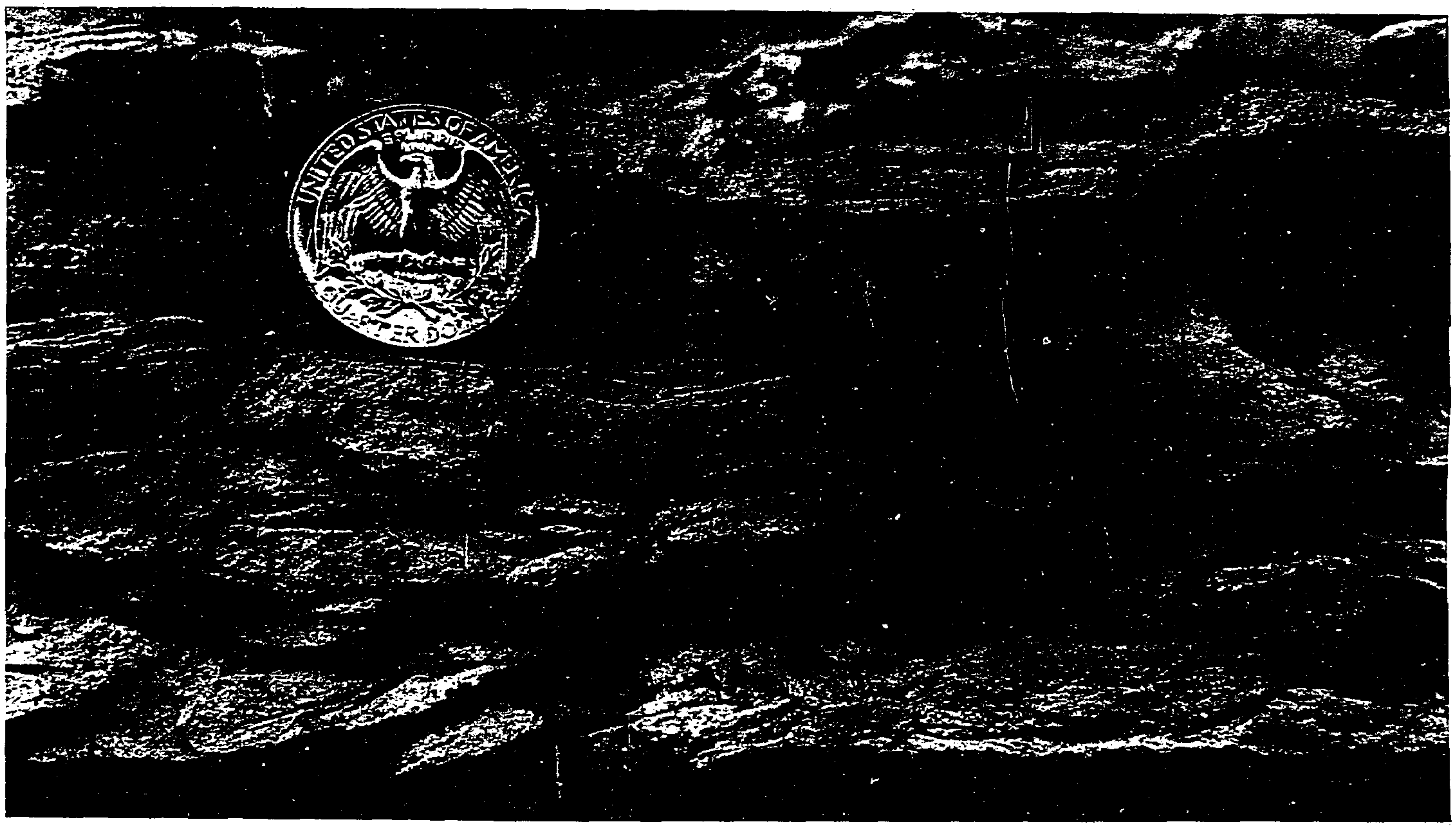

Figure 10. Photograph of form-discordant cross-lamination within a sandstone bed of the wavy-bedded facies of the Sundance Formation. The coin is 24 mm in diameter

Shale Member of the Sundance Formation, as defined by Imlay (1947). The thickness and frequency of the very fine-grained sandstone beds increase upward within the wavy-bedded facies, with a gradual upward transition from lenticular- to flaser-bedding (Reineck and Wunderlich, 1968).

Facies relationships

The sandstone facies overlies the coquina with a gradational to sharp, non-erosive contact. Typical vertical sections begin with a 1 m to 3 m thick coquina horizon separated from the underlying wavy-bedded facies by an erosion surface. The thick coquina horizon is overlain by 15-20 m of the sandstone facies in which several discontinuous coquina horizons less than 0.5 m thick may be present. Together, the sandstone and coquina facies comprise a tabular, laterally extensive unit of relatively constant thickness (cf., APPENDIX B).

Evidence of Tidal Influence

Perception of tidal current influence on the deposition of the Sundance Formation is not new. Stone and Vondra (1972) concluded that tidal currents were responsible for the deposition of a large scale trough cross-bedded oolitic calcarenite occurring near the top of the (Callovian) "lower Sundance" Formation in the Bighorn Basin. Their conclusion was based on the bipolar, bimodal distribution of paleocurrent data measured from the large scale trough cross-beds and the crests of symmetrical ripples developed on the cross-beds.

From outcrops in eastern and south-eastern Wyoming and western South Dakota, Rautman (1978) concluded that the "lower Sundance" Formation was deposited in a variety of tidally-influenced environments associated with a prograding barrier island complex. Shoreface and tidal channel sediments are overlain by back-barrier lagoon sediments in the vicinity of the Black Hills and by tidal flat deposits in south-eastern Wyoming. In both areas, the prograding shoreline sequence is overlain by the non-marine or supratidal Lak Member of the uppermost "Lower Sundance Formation (Rautman, 1978). The subaerial deposits of this Callovian prograding barrier shoreline are absent, as they are, for the most part, in the Oxfordian prograding barrier sequence described in this report. In both cases, the paucity of barrier-top sediments is attributed to reworking by tidal inlet channel processes.

The recently discovered (Elliott, 1984; Uhlir and Vondra, 1984; Uhlir, Vondra, Akers and Elliott, 1986) exposures of tidal bundles in the sandstone facies of the uppermost Sundance Formation (Figure 6) are the most compelling evidence for tidal influence during Sundance deposition. These exposures, located on the eastern margin of the Bighorn Basin (Figure 1) are remarkably well-preserved examples of structures that were first called bundles by Boersma (1969) when describing the internal stratification of tidal megaripples in the Westerschelde Estuary of the Netherlands. Kreisa and Moiola (1984, 1986) described sigmoidal tidal bundles in the Curtis Formation, a stratigraphic equivalent of the Sundance Formation in central Utah. Similar stratification has been described in ancient and modern sediments by Allen and Narayan (1964); Boersma (1967); Narayan (1971); Allen and Friend (1976a, 1976b); Nio (1976); Visser (1980); Allen (1981a, 1981b); Homewood and Allen (1981); Boersma and Terwindt (1981a, 1981b); Berg (1982); Siegenthaler (1982); Nio, Siegenthaler and Yang (1983); Allen and Homewood (1984); Teyssen (1984); Yang and Nio (1985); and Terwindt and Brouwer (1986). A cyclic variation in the thickness of the sets of large scale cross-stratification bounded by subordinate current reactivation surfaces should be demonstrable in tidal bundles. This thickness variation probably results from neap-spring variations in maximum tidal current velocity and a number of other factors which cause sediment transport rates in the dominant current direction (and therefore bedform migration rates) to vary markedly during the lunar month.

Tidal bundles of the Sundance Formation

Two exposures of the tidal bundles in the uppermost Sundance Formation display neap-spring set thickness variation. One outcrop exposes 37 consecutive bundles, the other, 27. Figure 11 depicts the neap-spring bundle thickness variation measured

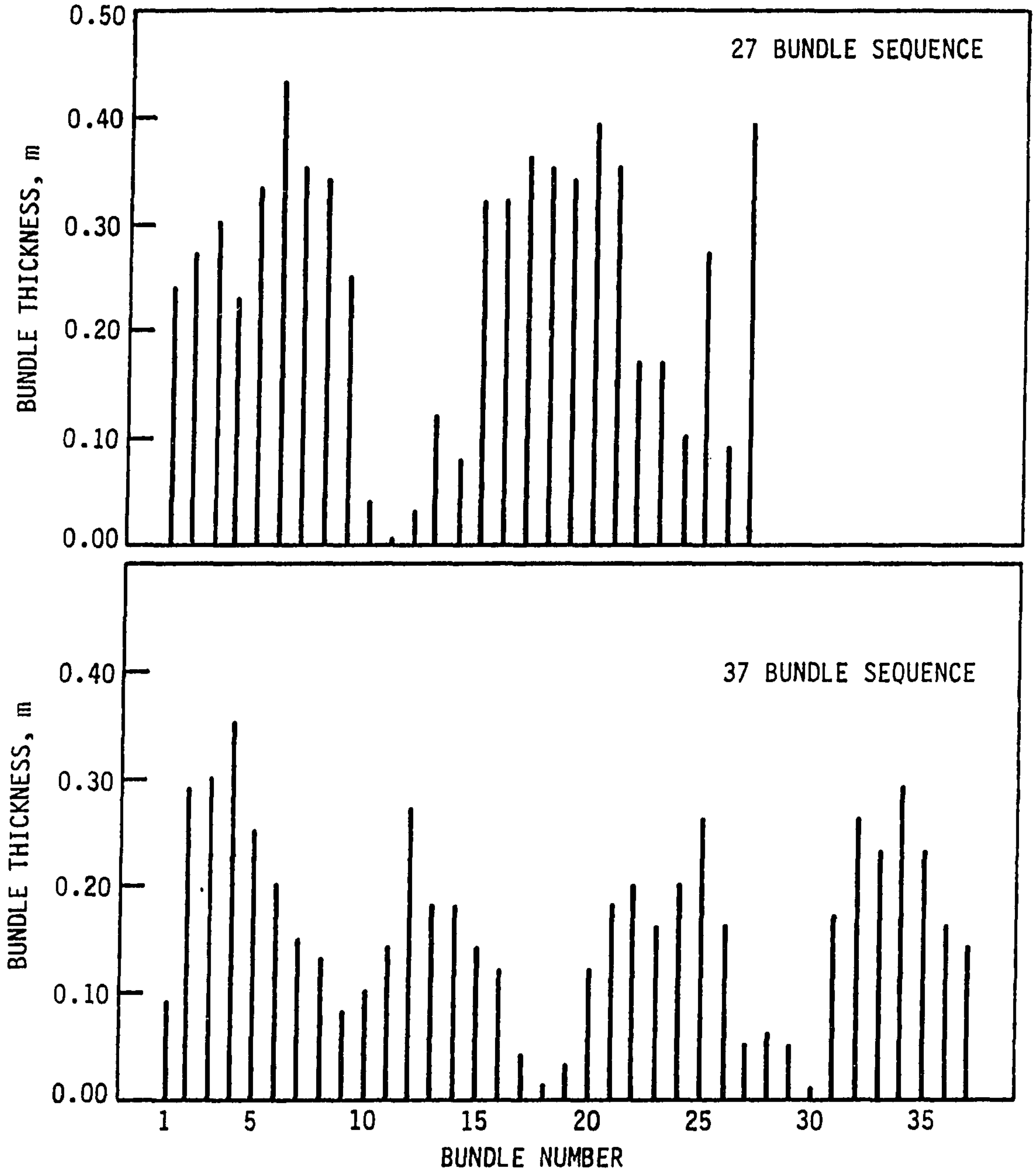

Figure 11. Bar graphs of tidal bundle thickness *versus* tidal bundle number showing the neap-spring variation in bundle thickness from two exposures of the sandstone facies at the SHELL 2 locality

perpendicular to the subordinate current reactivation surfaces at these outcrops. In these exposures, large scale trough cross-lamination sets are truncated by subordinate current reactivation surfaces that are overlain by subordinate current ripples 10 mm to 20 mm high, which are in turn overlain by a 1 mm to 3 mm thick mud drape. The subordinate current reactivation surfaces, subordinate current ripples and overlying mud drapes appear as the lighter-colored sigmoidal bands dipping to the left (south) in Figure 6 and can be seen in detail in Figure 7.

The large scale trough cross-lamination was most likely produced by a sinuous-crested megaripple (Type 2, as described by Dalrymple, Knight and Lambiase, 1978; Elliott and Gardiner, 1981) migrating to the south in the direction of the dominant tidal current. The inferred sequence of events for the development of the boundaries of the tidal bundles is as follows:

During the subordinate tidal current, the subordinate current reactivation surfaces formed, truncating some of the newly-deposited large scale trough foresets. As the subordinate current waned, subordinate current ripples migrating up the subordinate current reactivation surface became inactive. It is unlikely that the subordinate current reactivation surface and subordinate current ripples were developed by a current flowing in absolute (180°) opposition to the dominant current (Mowbray and Visser, 1984). However, the relatively-high foreset inclinations of the large scale trough cross-lamination (23° to 25°) and the ripple lamination (25°) indicate that the outcrop trend is nearly parallel to the megaripple and subordinate current ripple migration directions and that these directions were approximately opposed.

The subordinate current reactivation surfaces and subordinate current ripples cannot be backflow phenomena. The ripples are developed only on top of the subordinate current reactivation surfaces and are not "interwoven" (Boersma, Meene and Tjalsma, 1968) with the toes of the large scale foresets. The sigmoidal shape of the subordinate current reactivation surfaces implies that maximum erosion occurred near the crest of the megaripple during its subordinate current modification. The erosion associated with a lee-vortex backflow would be at a maximum considerably lower on the downcurrent side of the bedform, and a sigmoid-shaped erosion surface would not develop.

If the subordinate current reactivation surface and overlying current ripples were the result of dominant current backflow, their superposition could not be explained. In a situation where backflow is modifying the lee of a bedform, the maximum lee-side erosion occurs during the time of maximum dominant current velocity. As the dominant current wanes, large scale cross-laminae with interwoven backflow ripples are deposited. The backflow erosion surface does not truncate the whole set height of the large scale cross-laminae, and the backflow ripples are interspersed amongst the large scale cross-lamination. Backflow ripples are not restricted to positions overlying erosion surfaces as are the subordinate current ripples above the subordinate current reactivation surfaces in the tidal bundles of the Sundance Formation.

The 1 mm to 3 mm thick mud drapes, which overlie the subordinate current ripples, imply that the bedforms that produced the bundle sequence (and much of the sandstone facies in general) were migrating within a restricted environment (Allen, 1981a). As the rotary tide of open water encountered the coast, it was modified to ebb and flood currents of approximately opposite directions with high- and low-water stillstands in between. This flattening of the tidal current ellipse occurs in nearshore and estuarine environments (Allen, 1981a). Without the shoreline proximity, the rotary tidal currents would not slacken enough to allow suspension settling of the mud drapes. Thus the mud drapes, which are common throughout the sandstone facies, would not have been deposited in an unrestricted offshore environment. Even if the tidal current ellipse were sufficiently flattened to allow mud deposition in an offshore setting, the lack of protection from wave energy would make the regular preservation of mud drapes unlikely.

The fact that only one mud drape is preserved within each bundle-bounding surface may indicate that the megaripples into which the drapes were incorporated were intertidal bedforms. The bundle stratification sequence consists of large scale trough cross-lamination truncated by a subordinate current reactivation surface overlain by subordinate current ripples which are in turn overlain by a mud drape (Figure 7). If the bedforms were in an intertidal depth range, then the mud drape would have been deposited at the high-water stillstand; the bedforms being emergent at low-water. If this were the case, the subordinate current ripples, which immediately precede the mud drape deposition, were developed during the flood tidal current and the megaripples migrated during the (dominant) ebb. This scenario, though possible, is not probable. It is more likely that even though a mud drape may have been deposited directly above the large scale trough cross-lamination during the time of slackwater after the dominant tide, this post-dominant drape was removed during the subsequent development of the subordinate current reactivation surface.

The preservation of the post-subordinate tidal current mud drape is explained by its position in the lee (with respect to the dominant current) of the megaripple and by the deposition of the sand above the mud drape, but below the dominant current reactivation surface (Figure 7). The undulose laminations in the sand immediately below the dominant current reactivation surface may be the remnants of medium-scale bedforms that migrated down the lee of the megaripple at the very beginning of the dominant current.

The neap-spring bundle cycles (Figure 11) have a period of 9 to 13 bundles per cycle. This implies that the megaripples which formed the bundles were migrating in response to diurnal tides. In a diurnal tidal setting, there are roughly 14 days between successive spring tides or between successive neaps. If a complete record of the tidal current activity were preserved in the sediment, each cycle would consist of 14 bundles. Several reasons can be given to account for the incomplete nature of the preserved sequence. There may have been no dominant current megaripple migration during neap tide, so no new set of large scale trough cross-lamination was produced. Alternatively, the neap subordinate current may not have been strong enough to modify the megaripple, so a bundle-bounding subordinate current reactivation surface and subordinate current ripples were not developed. Or, the bundle-boundary may have been obscured by dominant current erosion during spring tide. The subordinate current reactivation surfaces, which are nearly concordant with the large scale trough foresets, are most easily observed when overlain by subordinate current ripples and a mud drape. If the subordinate current ripples and mud drape were eroded by the dominant spring tide, or somehow kept from forming, Formation. The cross-lamination sets typically have exterior forms suggestive of wave action (Figure 10) and have bimodal, bipolar foreset inclinations.

Cyclic zones of bioturbation, separated by undisturbed sediments constitute the sixth (and least important) tidally diagnostic characteristic of Raaf and Boersma (1971). Although the wavy-bedded facies is extensively bioturbated, it is difficult to demonstrate a regular pattern of biogenic structures. The sandstone facies is generally lacking bioturbation except within its upper 2 m.

Terwindt (1981) makes the diagnosis of tidal influence more specific, concluding that the occurrence of bidirectional foresets, subordinate current reactivation surfaces, waning-flow sequences and tidal bundles in the deposits of megaripples implies that the sediments were deposited in an inshore, mesotidal environment.

Estimation of Tidal Range

The large scale of the cross-stratification, both within the coquina and the sandstone facies implies that there was a significant tidal range along the late Sundance coast. The nature of the cross-stratification itself, particularly the presence of tidal bundles in the sandstone facies, implies the environment of deposition experienced at least mesotidal tidal ranges.

Modern and sub-recent tidal bundles have been described and analyzed by Boersma (1969); Visser (1980); Terwindt (1981); Boersma and Terwindt (1981a, 1981b); Berg (1982); Siegenthaler (1982); Nio, Siegenthaler and Yang (1983); Mowbray and Visser (1984); Yang and Nio (1985); and Terwindt and Brouwer (1986). Tidal bundles, bidirectional foreset inclination, reactivation and waning-flow structures are some of the principal diagnostic components of inshore mesotidal deposits (Terwindt, 1981). All of these structures are found in the sandstone facies of the uppermost Sundance Formation.

Inlet spacing along barrier coastlines is inversely proportional to the tidal range (Hayes, 1975). Microtidal coasts have their barriers infrequently interrupted by tidal inlets. Macrotidal bays and estuaries are in effect, large, but relatively non-migratory tidal inlets without the associated barrier islands. Mesotidal coasts have the highest frequency of interbarrier tidal inlets, and these inlets are typically migratory. Thus a mesotidal environment is most probably responsible for developing the laterally extensive tidal inlet and inlet-lag deposits of the Sundance sandstone and coquina facies, respectively.

Quantitative estimate

The tidal bundles of the uppermost Sundance Formation were developed principally under the influence of asymmetric, probably diurnal tidal currents. The diurnal nature of these currents is deduced from the near 14 bundles per neap-spring cycle. This determination allows an estimate of the rate of megaripple migration to be made. The rate of bedform migration is proportional to the tidal current velocity. The maximum tidal current velocity is especially significant (Allen and Friend, 1976a, 1976b). Thus, the paleotidal range of bundle-forming environments may be estimated from the dimensions of the cross-stratification of the bundles.

A quantitative estimate of the tidal range that existed during the development of the tidal bundles of the uppermost Sundance Formation is made in Uhlir, Akers and Vondra (submitted). Assuming that the tides were diurnal, they estimate that the mean tidal range was 3.7 m during the deposition of the 27-bundle sequence and 1.3 m for the 37-bundle sequence. If the tides are assumed to have been semi-diurnal (twice daily) during the development of the bundled cross-stratification, the sediment transport rates would have been roughly twice as rapid as those calculated for the diurnal setting. Assuming semi-diurnal tides, mean tidal ranges of 6.3 m and 2.2 m were calculated for the 27-bundle and 37-bundle sequences, respectively (cf., APPENDIX C).

Tidal Inlet Sequence of the Uppermost Sundance Formation

The sequence of textures, lithologies and sedimentary structures deposited by the lateral migration of tidal inlets has been a concern of a number of studies: Price (1963); Hoyt and Henry (1965,1967); Davies, Ethridge and Berg (1971); Kumar and Sanders (1974); Greer (1975); Barwis and Makurath (1978); Hubbard, Oertal and Nummendal (1979); and Berg (1982). An observation noted by many of these workers is the similarity between the deposits of migrating tidal inlets and the sequence left by meandering stream systems. Both of these environments result in a coarse-grained lag with an erosive base overlain by sands with cross-stratification that decreases in scale upward. There is an upward increase in the amount of upper-stage horizontal lamination within these sands as well. The fluvial channel sequence is overlain by overbank silts and clays. The tidal inlet sequence is capped by estuarine or lagoonal silts and clays.

In both cases, it is the incised nature and lateral migration of the channel that leads to the preservation of the deposits. This is particularly true in the case of tidal inlets, which may incise several tens of meters below sea level (Price, 1963; Hoyt and Henry, 1965, 1967; Kumar and Sanders, 1974; Greer, 1975) giving tidal inlet deposits very good preservation potential.

The coquina and sandstone facies of the Sundance Formation conform well with the tidal inlet sequences described from both modern and ancient sediments. The major horizons of the coquina facies represent the lag of the tidal inlets. The coarse and fragmental texture of the coquina facies and its erosive base resulted from the high current velocities that existed in the deepest part of the inlet channel.

The lateral migration of the tidal inlets resulted in the development of lateral accretion surfaces or epsilon cross-stratification (Allen, 1963) within the coquina facies (Figure 9). Paleocurrent directions measured from the trough axes of the overlying cross-laminated sandstone tend to be normal to the dip of the lateral accretion surfaces in the coquina at a given locality.

The coquina facies has the most potential for utility in regional paleogeographic syntheses. The beds of fragmental coquina more than half a meter thick were developed in very high energy environments. The throats of tidal inlets, where the channel is deepest (landward of ebb tidal deltas, seaward of flood tidal deltas, if present) are the most likely paleo-environments for the development and deposition of the thick beds of fragmental coquina. Back-barrier tidal inlet channels may be quite sinuous, but interbarrier inlet throats tend to be quite straight. Inlet throats trend roughly normal to the shoreline, and migrate in shore-parallel directions (Frey and Howard, 1986). Thus, the lateral accretion directions measured from the coquina facies of the Sundance Formation may be considered an

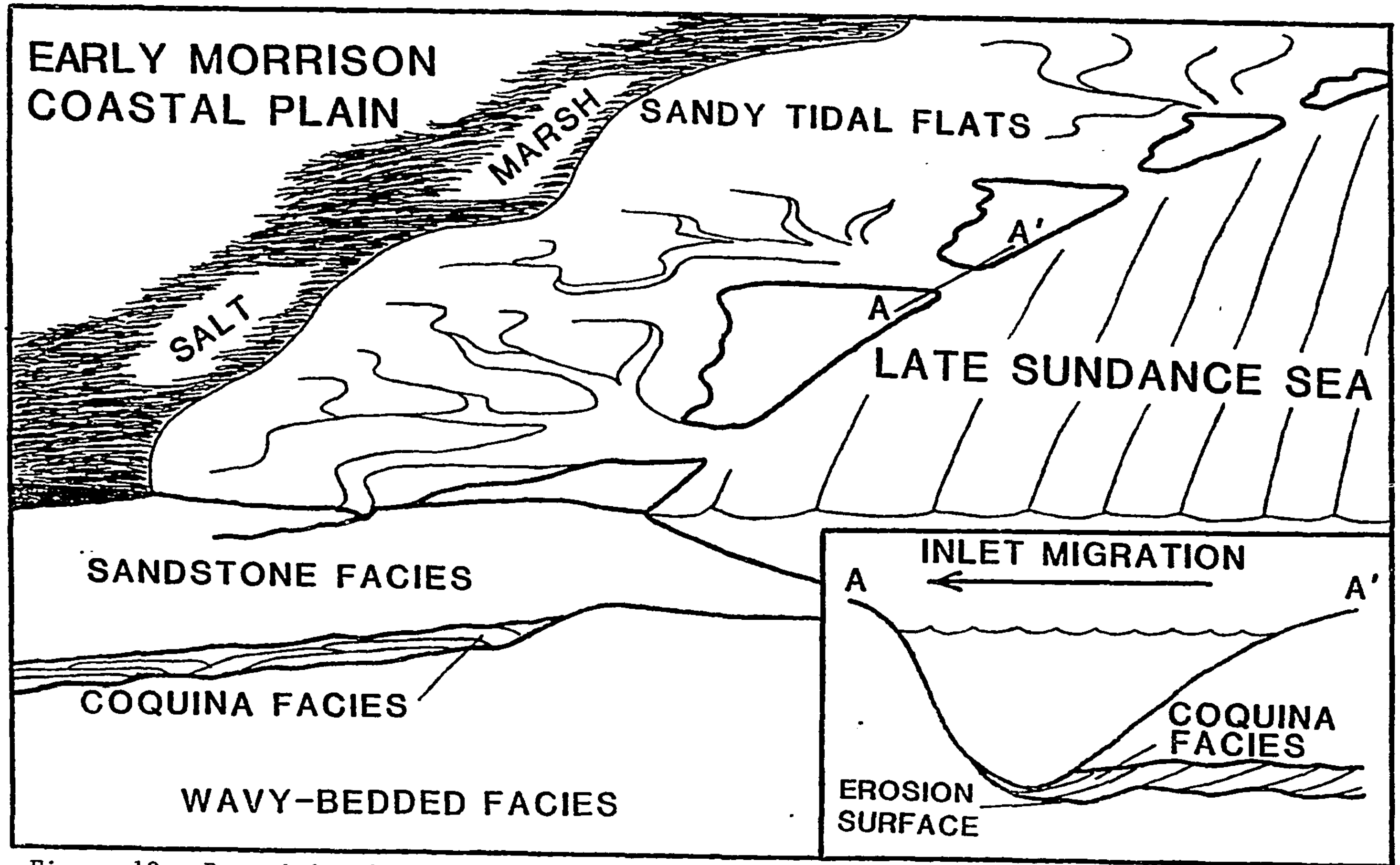

Figure 12. Depositional Model for the uppermost Sundance and basal Morrison formations in north-central Wyoming. Cross-section A-A' depicts the facies relationship created by the lateral migration of interbarrier tidal inlets

approximation of the trend of the Late Jurassic shoreline.

Although sea level rose during the Oxfordian (Vail, Hardenbol and Todd, 1984) the lingoid late Sundance seaway (Peterson, 1972; Imlay, 1980) withdrew as the early Morrison coastal plain prograded to the north (Moritz, 1951). When the shoreline was in north-central Wyoming, mesotidal barrier islands and the interbarrier tidal inlets migrated along this coast in response to longshore currents (Figure 12). That this coastline trended east-west is supported by the generally east-west lateral migration directions measured from the coquina facies (Figure 13). The combination of lateral inlet migration with the general withdrawal of the late Sundance sea caused the coquina and sandstone facies to be deposited as a tabular, laterally-extensive tidal inlet sequence (Figures 4, 12).

Trough cross-bedding also occurs in the coquina facies, generally toward the top of the unit. The trough axes at a given locality tend to be roughly normal to the dip of the lateral accretion surfaces (e.g., Figure 14). This suggests that in addition to the shore-parallel inlet accretion, there was a shore-normal transport of coarse-grained material near the base of the inlet channels.

The advance of the early Morrison coast is also recorded in the inner shelf and lower shoreface sediments of the wavy-bedded facies, into which the coquina and sandstone tidal inlet sequence

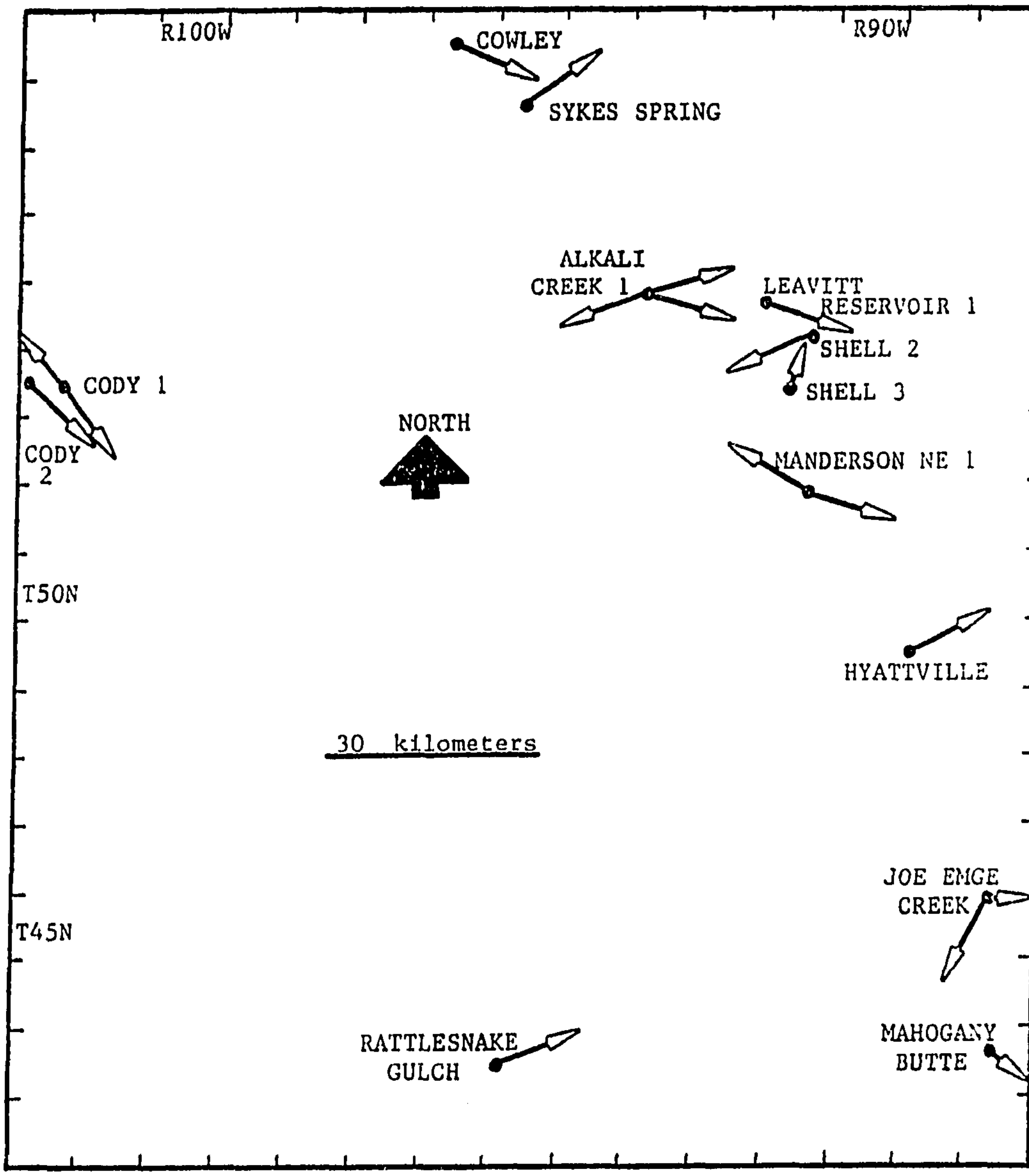

Figure 13. Plot of lateral accretion directions measured from the coquina facies of the uppermost Sundance Formation at exposures in the Bighorn Basin of Wyoming. The arrows point in the maximum dip direction of epsilon cross-stratification surfaces. The exposures are located by section, township and range notation in APPENDIX A

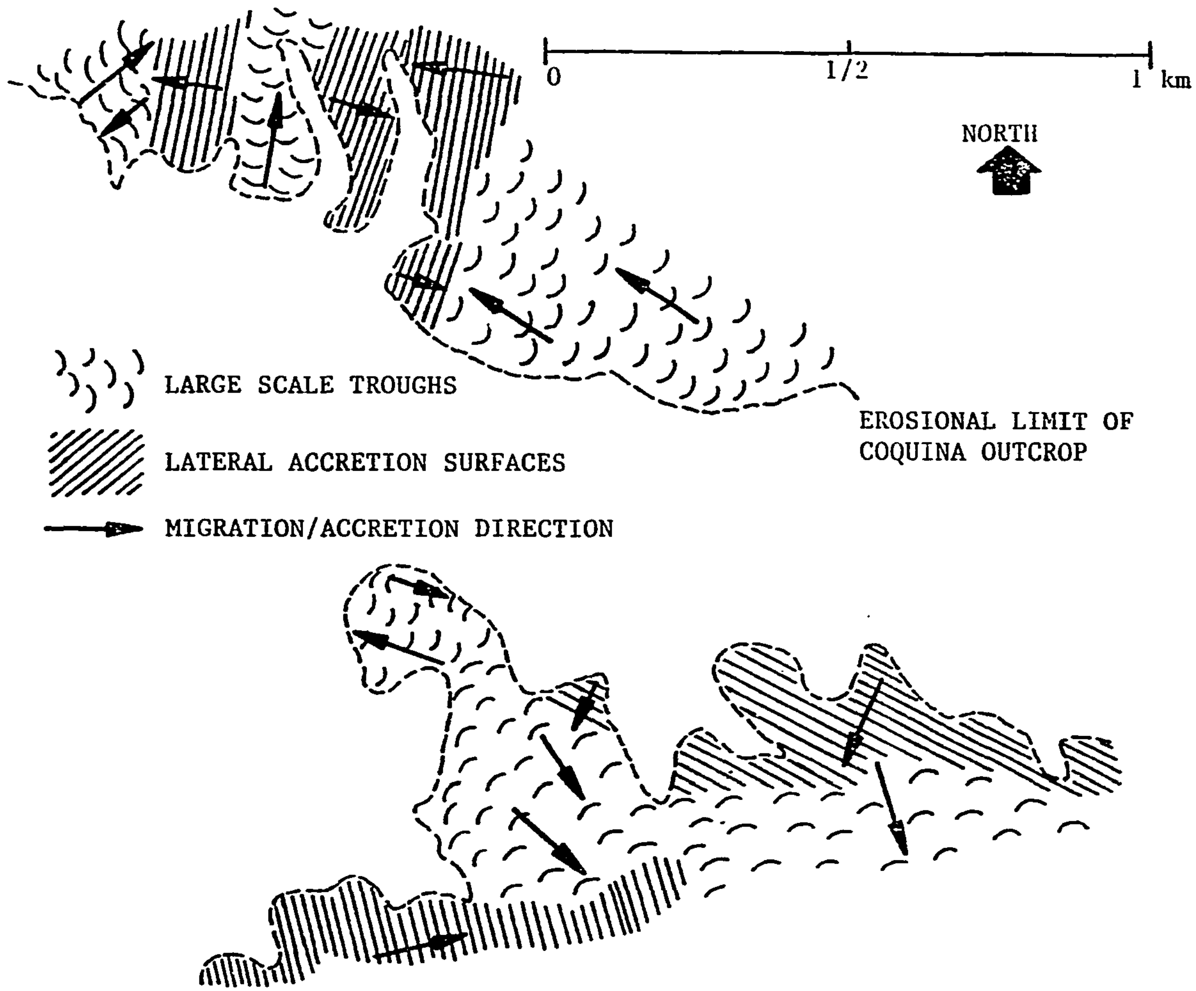

Figure 14. Map of lateral accretion surfaces and large scale troughs in a laterally-extensive exposure of the coquina facies of the Sundance Formation in the vicinity of the ALKALI CREEK 1 locality. Coquina stratum dips 0.5° to N40E

is incised. In the wavy-bedded facies, the upward transition from lenticular, to wavy, to flaser bedding resulted from the approach of the shoreline through time. In many places, the top of this sequence is absent, the flaser bedded units having been cut out by erosion at the base of the tidal inlets as the barrier complex prograded over the lower shoreface deposits.

A number of plausible interpretations may be presented for the development of some of the primary sedimentary structures in the sandstone facies. The large scale trough cross-lamination of the sandstone facies could have been developed in the deeper parts of the inlet channels (Kumar and Sanders, 1974). It also could have formed on back-barrier shoals (Boersma, 1969; Raaf and Boersma, 1971; Boersma and Terwindt, 1981a, 1981b) or in channels within such shoals (Nio, Berg, Goesten and Smulders, 1980). The horizontal lamination, which is very common in the upper part of the sandstone facies, could have formed in very shallow water within a tidal inlet channel (Kumar and Sanders, 1974) on the tops of back-barrier shoals, tidal deltas, or sandy tidal flats. Where the horizontally laminated sands are underlain by a thin (less than 0.5 m thick) coquina unit, composed of relatively whole shells, the tidal flat setting is suggested. In these cases, the thin coquina unit represents the lag of tidal creeks meandering within the sand flats in the manner described by Straaten (1950, 1954); Klein (1963); and Reineck (1967).

It is likely that the structures of the sandstone facies developed in some, or even all of the subenvironments of the mesotidal barrier coastline. However, the high preservation potential of tidal inlet deposits makes them likely to dominate such an assemblage, particularly in the lower parts of the sequence. Brenner and Davies (1974) noted the similarity between tidal inlet sequences and the uppermost Sundance Formation, but then went on to develop their storm-dominated offshore bar model. The reason for their rejection of the barrier coastline hypothesis is the lack of the subaerial (barrier top) components of the inlet sequence in the Sundance sediments. However, it is this subaerial portion of the sequence that stands the least chance of preservation (Hoyt and Henry, 1965, 1967; Barwis and Makurath, 1978).

In rare instances, the upper portion of the sandstone facies is characterized by very broadly swaley lamination capped by a massive, very fine-grained sandstone with a very low percentage of glauconite (Figure 15). The writer interprets the swaley laminated sandstone to represent upper shoreface deposits. The overlying massive sandstone is probably from eolian, barrier-top dunes. This eolian interpretation is supported by the lithologic similarity of the massive sandstone to much thicker, more clearly eolian deposits which overlie the Sundance Formation in parts of central Wyoming (Uhlir, 1986). The Upper Jurassic eolian

Figure 15. Photograph of an exposure of the sandstone facies of the uppermost Sundance Formation in the vicinity of the NORTH EMBLEM RESERVOIR 5 locality. The sandstone facies exhibits atypical swaley (upper shoreface) lamination capped by lighter-colored massive (eolian?) sandstone bed 1.2 m thick. This stratification sequence may represent the subaerial deposits of a barrier island

sandstones of central Wyoming most likely represent dune fields developed on the prograding Morrison coastal plain. These eolian sandstones are very well-sorted and often quite friable, which lends them a massive appearance at some outcrops.

Discussion of Other Depositional Models

Few will argue against the terrestrial nature of the Morrison Formation, yet if the sandstones and coquinas of the Sundance Formation, which conformably underlie the Morrison, are offshore sand ridge deposits, then the near- and inshore deposits of this marine to terrestrial transition are inexplicably absent. Offshore sand ridges are relatively stable, discrete, linear sand bodies (Off, 1963; Swift, Stanley and Curray, 1971; Swift, 1975; Kenyon, Belderson, Stride and Johnson, 1981) with a regular crest spacing that may be recognized in ancient deposits (Off, 1963). No such pattern is discernible in the tabular coquina and sandstone facies of the uppermost Sundance Formation. The tabular horizons of the coquina facies are often traceable for tens of kilometers in outcrop. Yet sand ridges (Off, 1963; Swift et al., 1971; Swift, 1975; Kenyon et al., 1981) and sand wave fields (McCave, 1971; Langhorne, 1973; Allen, 1980b) do not migrate rapidly compared to tidal inlets. Shell accumulations within such offshore sand bodies could hardly be expected to be tabular.

When shell accumulations are associated with offshore sand bodies, they most commonly occur as shell pavements in between sand ridges or sand wave fields, not actually incorporated into the sand accumulations (Belderson and Stride, 1966; Kenyon et al., 1981; Wilson, 1982). If scour in the lee vortex of sand waves (Allen, 1965) did cause a shell accumulation, it is very unlikely that such an accumulation would achieve a thickness comparable to that of the coquina facies of the Sundance Formation (often greater than 2 m thick). Such a thickness is also improbable for a shell hash left behind in the wake of a storm.

Neither the storm (Brenner and Davies, 1973, 1974) or storm, tide and lee-vortex (Brenner et al., 1985) models explain the large scale cross-stratification within the coquina facies. This cross-stratification, in conjunction with the typically extreme degree of shell fragmentation, suggests a continuous high-energy environment, as would be found at the base of a tidal inlet.

A tidal estuary is a plausible environment of deposition for the coquina and sandstone facies. In an estuary model (e.g., Frey and Howard, 1986) the coquina would be considered a tidal inlet lag, just as it is in the barrier coastline model. However, the inlets would be between estuarine shoals, rather than in between barriers. The evidence which favors the barrier coastline model over the tidal estuary model comes principally from exposures of great lateral extent (e.g., Figure 14). It is these exposures that best display the tabular, laterally-extensive geometry of the coquina facies. If the coquina is estuarine, a great deal of lateral migration of the intershoal inlet channels is necessitated to explain the tabular geometry of the inlet lag. If the intershoal channels were not actively migratory, then lenticular, rather than tabular bodies of coquina would be anticipated.

Though rarely preserved, the presence of patches of shoreface and eolian strata at the top of the sandstone facies (Figure 15) also lends support to the barrier coastline model. The undulous lamination of shoreface sediments is developed by the swash and backswash of waves against the shore. Swash/backswash processes are most significant where the shoreline facing wave approach is relatively linear and continuous. Barrier coastlines are much more linear and continous (interrupted only by tidal inlets) than tidal estuaries. Eolian dunes are common on top of barrier islands, but rare within estuaries. The large supratidal areas necessary for the development and migration of eolian dunes are, in general, not present within estuaries.

Summary of Interpretations of Depositional Environment

The sandstones and coquinas of the uppermost 15-20 m of the Sundance Formation represent the deposits of a Late Jurassic prograding, tide-dominated barrier coastline. Tidal bundles measured within the sandstone facies of this sequence record the neap-spring variation in migration rates of sinuous-crested megaripples. The cyclicity of this neap spring variation implies that the tides were most likely diurnal during the tidal bundle development.

The bulk of the coquina and sandstone facies was deposited in association with interbarrier tidal inlets. Subordinate current reactivation surfaces, tidal bundles, and mud drapes in the sandstone facies suggest deposition of the unit within a nearshore or inshore setting. The fragmental, large scale cross-stratified coquina facies is best explained as the lag of laterally migrating tidal inlets. There is a striking similarity between the coquina and sandstone facies of the Sundance Formation and sediments of modern tidal inlet sequences.

Offshore sand body models do not explain the conformable stratigraphic relations between the Sundance and Morrison formations in north-central Wyoming. The tabular, laterally-extensive geometry of the Sundance sandstone and coquina facies is like that expected from the deposits of barrier coastline with laterally migrating tidal inlets (e.g., Hubbard et al., 1979). Such a geometry would not be anticipated if these were truly offshore deposits.

CHAPTER IV. TECTONIC IMPLICATIONS

Summary

Recent studies of the development and sedimentary infilling of foreland basins strongly support the hypothesis that the Oxfordian seaway of the western interior of North America is principally of tectonic origin. The seaway formed by downbowing of the North American craton in respose to the load of the Cordilleran thrust belt. During the Late Jurassic, the frontal thrusts of this orogen occupied a belt that trended generally northward, from western Utah to eastern British Columbia. Attaching a name to this Late Jurassic tectonic activity is difficult. Compared to the thrust loading and foreland basin development of the Late Cretaceous, the Jurassic activity is modest. Some workers (e.g., Allmendinger and Jordan, 1981) consider that these motions represent the initiation of the Sevier orogeny, while others (e.g., Heller et al., 1986) vehemently reject this notion.

Field evidence observed during the course of the research for this dissertation indicates that positive structural elements were active within the central and north-central parts of Wyoming during the Late Jurassic. The positions of these structures are coincident with similar, late Paleozoic highs and with mountain ranges and arches of Laramide age. The concept of a tectonically quiescent "Wyoming shelf" (N.B. Figure 3) during the deposition of the Sundance Formation is outdated. The regression which controlled the deposition of the uppermost Sundance Formation was driven mainly by tectonic events within the western interior.

The Late Jurassic Foreland Basin of North America

Evidence for the tectonic origin of the Late Jurassic epicontinental seaway is clearest in Canada. In the Alberta trough, deposition of the (marine Oxfordian) Green beds and Passage beds of the uppermost Fernie Formation is clearly linked to the emplacement of the thrust sheets of the early Columbian orogeny (Poulton, 1984). This conclusion is an outgrowth of one of the first models for the isostatic response of a foreland to tectonic loading, developed by Price (1973) in the Alberta foreland. Also using the Late Jurassic to Eocene Alberta foreland basin as his primary example, Beaumont (1981, p. 292) proposed a general model for the development of foreland basins stating that they form "in response to passive loading by supralithospheric mass loads superimposed during formation of the fold-thrust belt."

In the United States, implications that the Upper Jurassic deposits of the western interior were deposited in a foreland basin have met with more resistance. Brenner (1983) in one of the most recent paleotectonic syntheses of the Late Jurassic, avoided a direct confrontation with this issue. He (Brenner, 1983, p. 122) mentioned that the Nevadan subduction-arc complex may have been "the locus of activity that led to widespread uplift and associated thrusting west of the Late Jurassic interior sea...." Armstrong and Oriel (1986, p. 248) acknowledged tectonic activity west of the foreland basin during the early Late Jurassic, stating "the high on the west rose, again spread eastward, and shed detritus now found in the Preuss and Stump [formations]." Armstrong and Oriel (1986) made no direct statement linking thrusting with the rise of this "high." They (Armstrong and Oriel, 1986) referred to the deeper, western margin of the Jurassic seaway as a "geosyncline", thus refraining from making any implications as to its development.

Figure 16 shows the thickness and sedimentary facies variations of the rocks of the Jurassic System in the western interior. The marked thickening of the Jurassic section in central Utah, eastern Idaho and western Wyoming defines the region called the "Utah-Idaho trough" by Peterson (1972). Dickinson (1976, p. 1275) expressed uncertainty over whether this trough "was an incipient foreland basin." Later findings lend support to the hypothesis that the development of this trough corresponds to the start of an early phase of Sevier deformation (Wiltschko and Dorr, 1983). This trough lies immediately to the east of the position of the "Hansel" thrust plate, which was emplaced during "Middle to Late Jurassic" time (Allmendinger and Jordan, 1981, p. 311).

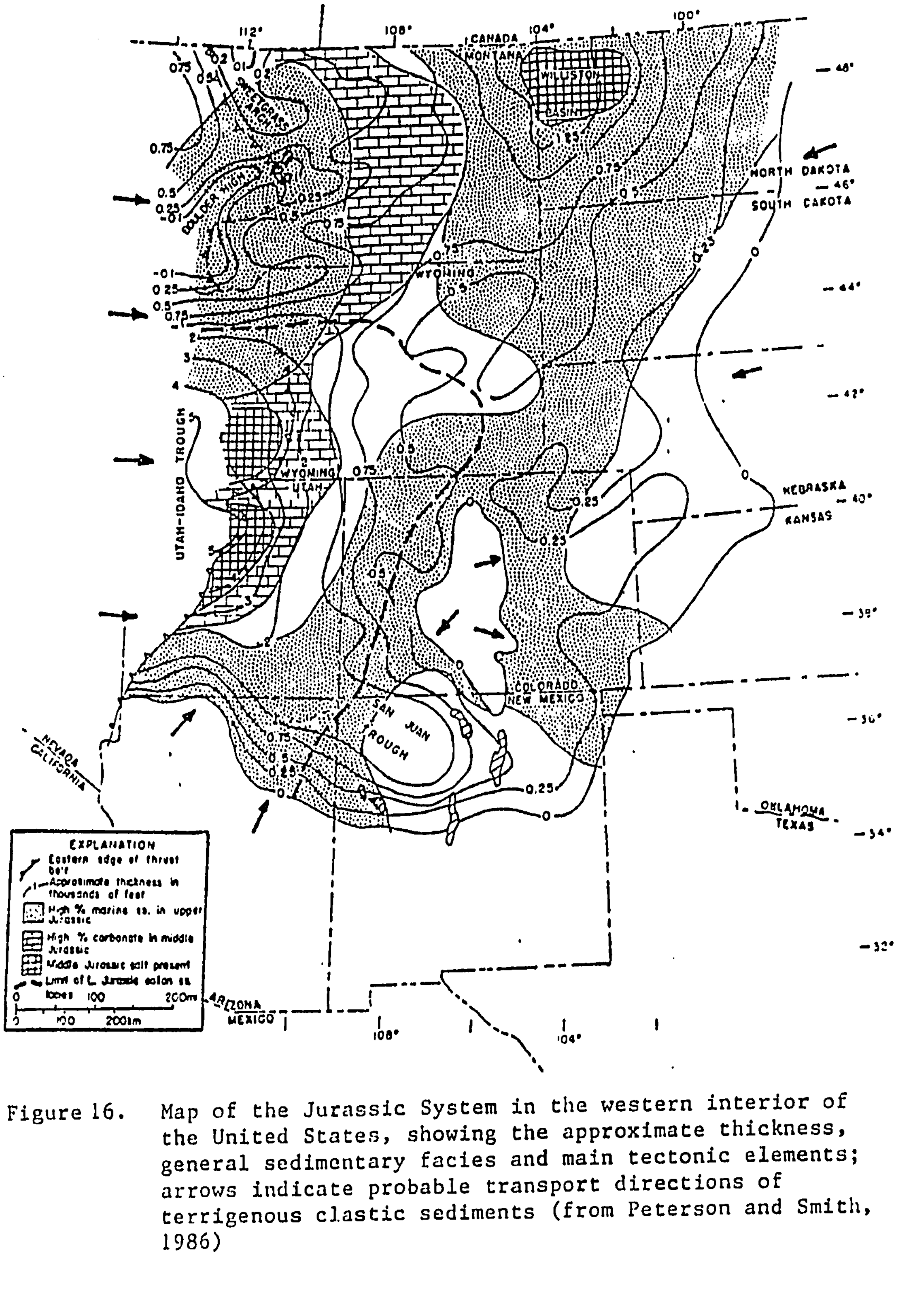

Figure 16. Map of the Jurassic System in the western interior of the United States, showing the approximate thickness, general sedimentary facies and main tectonic elements; arrows indicate probable transport directions of terrigenous clastic sediments (from Peterson and Smith, 1986)

Considering the whole of Figure 16, the thickness variation of the Jurassic strata of the western interior strongly suggests that an active orogenic belt existed immediately adjacent to the western margin of the depositional basin. It appears that the passive crustal loading associated with this orogenic belt caused the North American craton to subside. The greatest subsidence was within the Utah-Idaho trough, that part of the craton immediately adjacent to the thrust front. The general eastward thinning of the Jurassic strata reflects the diminishing effect of the tectonic load with distance from the thrust front. These relations fit Beaumont's (1981) model without difficulties. It is the contention of the writer that the Jurassic deposits of the western interior, particularly the Upper Jurassic rocks, were deposited within a foreland basin of the Sevier orogenic belt.

This contention conflicts with the conclusions of Heller _et al._ (1986, pp. 388-389) who asserted that "Sevier deformation was probably no older than late Early (i.e., middle) Cretaceous age." Heller _et al._ (1986) dated the upper member of the Ephraim Conglomerate as Aptian (late Early Cretaceous) on the basis of paleontological evidence. They (Heller _et al._, 1986) contended that this upper member of the Ephraim Conglomerate is the first "synorogenic" deposit shed from the Sevier thrust front.

From subsidence history curves of the Sevier Foreland area, Heller _et al._ (1986) concluded that Late Jurassic subsidence was the result of tectonic events that occurred too far west to be included in the Sevier orogenic belt. One of the tectonic agents they (Heller _et al._, 1986, p. 390) considered as a possible cause of Late Jurassic subsidence was "the emplacement of thrust plates in Nevada and northwestern Utah (e.g., Allmendinger _et al._, 1984)." This is the emplacement of the "Hansel plate" described by Allmendinger and Jordan (1981) and discussed above.

Apparently, Heller _et al._ (1986) used a much more restricted definition of the areal extent of the Sevier orogenic belt than that employed by Allmendinger and Jordan (1981) and Allmendinger _et al._ (1984). There are marked similarities in the strike, mode and direction of emplacement of the Hansel plate and the younger (Paris, Crawford, etc.) thrust sheets to the east. On this basis, The writer follows Allmendinger and Jordan (1981) and Allmendinger _et al._ (1984) in considering the Hansel plate emplacement to be an early Sevier event.

Structures within the Late Jurassic Foreland Basin

Dark colored chert clasts in the uppermost Sundance Formation

The areal distribution of dark chert clasts in the uppermost Sundance Formation suggests that areas of positive relief existed in north-central Wyoming during the Oxfordian. These Late Jurassic positive elements were located in the area of the Bighorn Mountains, a principally Laramide-age range. These structures were most likely either islands within or hills along the eastern margin of the regressing Oxfordian sea.

In most respects, the Late Jurassic positive structures of north-central Wyoming were quite similar to the coeval Belt Island of southwestern Montana, described by Imlay (1947). However, a very significant difference exists in that a major Laramide mountain range did not develop in the Belt Island area. Because the Belt Island was not overwhelmed by the later development of Laramide-age mountains, the proximal conglomerates shed from its margins have been preserved. In contrast, the overprint of the Bighorn Mountains, and the subsequent erosion of the 100 km wide band of Jurassic sediments above the range (Figure 1) has removed the most obvious evidence of the Late Jurassic highs in north-central Wyoming.

The largest chert clasts in the Sundance Formation of north-central Wyoming are well rounded, subspherical pebbles incorporated into 1-4 m thick beds of fragmental, arenaceous biosparite, which is referred to as the "coquina facies" in the DEPOSITIONAL ENVIRONMENT chapter of this dissertation. The percentage and grain size of dark chert clasts in the coquina facies decreases with distance from the Bighorn Mountains. Pebble-size clasts of chert are common in exposures of the coquina facies along the western and southwestern flanks of the Bighorn Mountains (sections 25-32, 51, 58, 59 of APPENDIX A). Only sparse, sand-sized clasts of chert occur in the coquina facies at outcrops 30-50 km west of the mountain front (sections 5-24, 38-49). Sand-sized dark chert clasts were noted in the coquina facies at sections 60-63 on the southeastern flank of the Bighorn Mountains.

The chert clasts were probably derived from the erosion of upper Paleozoic units (the Permian Phosphoria, Goose Egg and/or the Pennsylvanian Tensleep formations) on the crests of the Late Jurassic structures. The upper Paleozoic provenance is suggested by the color and banding of the chert clasts and the absence of chert of this color in the early Mesozoic units which were deposited before the Sundance Formation. The chert clasts range in color from tan to dark brown and black. Some granule- and larger-sized clasts exhibit 1 mm wide banding. Typically, milky white bands alternate with dark brown bands in this variety of chert. These colors and banding are typical of the chert derived from the carbonate and chert facies of the Phosphoria Formation described by Peterson (1980). Some of the lower Mesozoic units of central Wyoming (notably the Gypsum Spring Formation) contain chert, but this chert is not typically brown or black.

Dark colored chert clasts of upper Paleozoic provenance also occur in the Swift Formation and the upper part of the Sundance Formation of western Montana and Wyoming, respectively (Brenner and Davies, 1973, 1974). This chert was most likely derived from erosion of the early Sevier thrust sheets which lay to the west of the Oxfordian seaway.

Eolian sandstone of the Morrison Formation, central Wyoming

In many parts of central Wyoming, a fine- to very fine-grained quartz arenite overlies the glauconitic sublitharenite of the sandstone facies of the uppermost Sundance Formation. Eolian activity was largely responsible for the deposition of this unit (Uhlir, 1986; Weed and Vondra, 1987).

Love (1958) called this unit the "yellow sandstone member" of the Morrison Formation and suggests its correlation with the Unkpapa Sandstone Member of the Morrison Formation of the Black Hills region. Love (1958) assigned the unit to the Morrison Formation from the presence of freshwater gastropods in the sandstone in some areas. He (Love, 1958) discussed the abrupt change from the glauconite-rich uppermost Sundance sandstones to the yellow sandstone member, which contains only traces of glauconite.

Mirsky (1962) was the first to suggest that this unit was of eolian origin. However, he considered the unit to be eolian only at one of his localities (section 62 of APPENDIX A, this report). He (Mirsky, 1962, p. 1675) stated that "The deposit is restricted in extent...at least the lower part of the Morrison may have originated as coastal dunes marginal to the retreating Sundance sea, or as dunes on a floodplain." Douglass (1984) described an "eolian dune sand" in the lower Morrison in the vicinity of Thermopolis, Wyoming (Figure 1).

Work in the Black Hills by Szigeti and Fox (1981) on the Unkpapa Sandstone Member of the Morrison Formation shows the distinct similarities between the Unkpapa Sandstone Member and the lower Morrison eolian sandstone of central Wyoming. Both of these units share the same: stratigraphic position (at or very near the base of the Morrison Formation); lithology (fine- to very fine-grained quartz arenite); depositional process (eolian); transport direction (generally northward); and regional thickness variation (thinning towards the north).

Regional paleogeography may have had a significant influence on the wind patterns in Wyoming at the onset of Morrison deposition. The Oxfordian seaway lay immediately adjacent to the early Morrison coastal plain. The eolian sandstone unit was deposited at the margins of this coastal plain. The predominantly northward eolian transport recorded in the lower Morrison sandstone unit of central Wyoming may be the result of winds that blew from the coastal plain towards the seaway (Uhlir, 1986).

The presence of anomalous patches of eolian sandstone within the fluvial mudstones which form the bulk of the Morrison Formation suggests that topographic irregularities existed on the lower Morrison coastal plain. The eolian sandstone was deposited in the southern Bighorn Basin, the Wind River Basin and the southern Powder River Basin (Figure 17). This distribution of

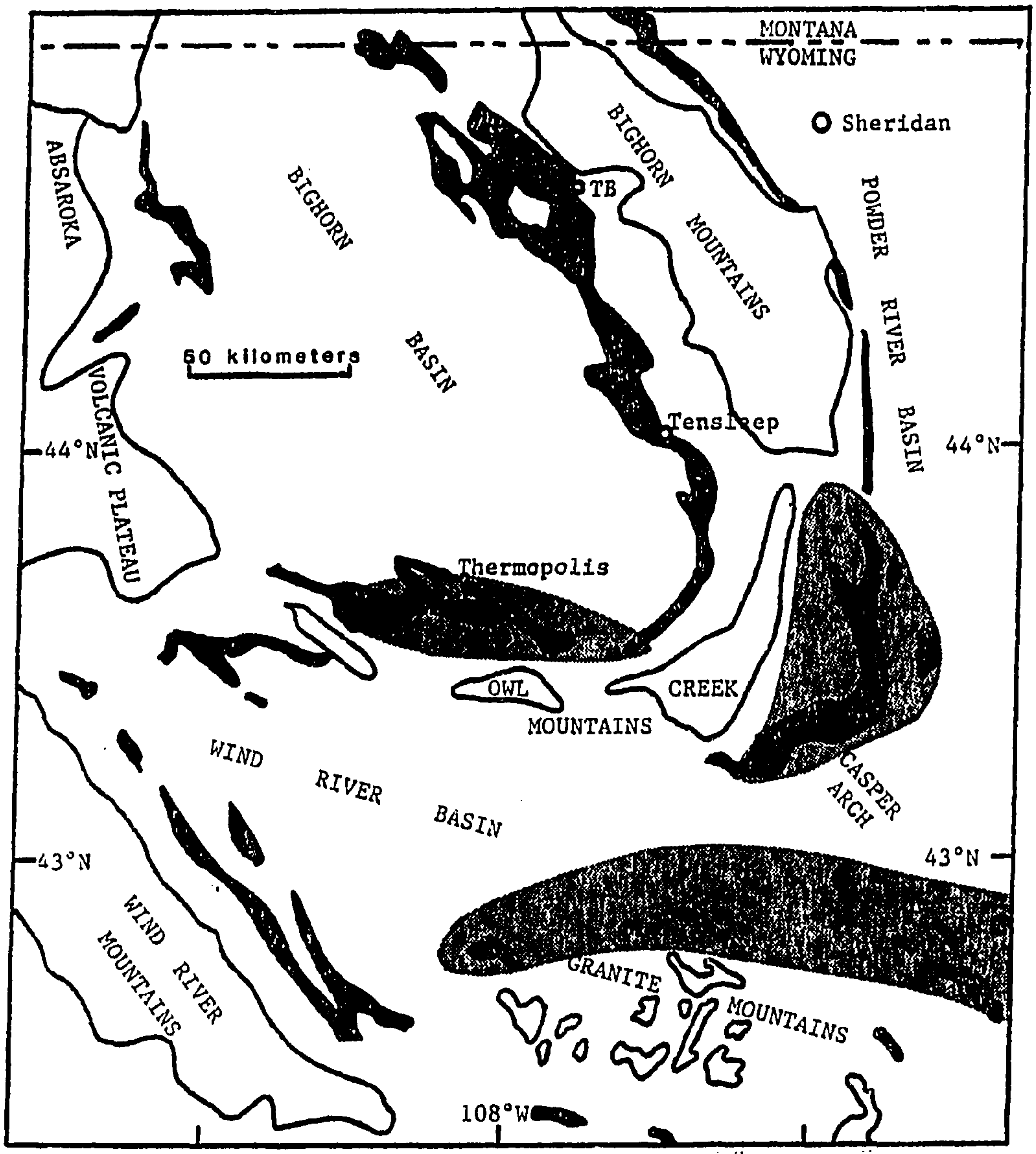

Figure 17. Map of the distribution of eolian sandstone deposits (shaded areas) within the lower part of the Morrison Formation in central Wyoming. Outcrops of Upper Jurassic and Lower Cretaceous rocks are shown in black. The eolian sandstone distribution is speculative in areas lacking outcrop control. Base map modified from Renfro and Feray (1972)

eolian sandstone deposits, considered together with the unit's northward thinning and transport direction, imply that the topographic irregularities on the Morrison coastal plain were located in the positions of the Owl Creek Mountains, the Granite Mountains and the Casper Arch, respectively.

The eolian sandstone was most likely derived from sandstones of the Sundance and older formations. Excluding the eolian unit, the lower part of the Morrison Formation in central Wyoming does not contain sufficient sandstone for it to be considered a probable source of the eolian sand. To expose the pre-Morrison strata to winnowing, the topographic irregularities on the early Morrison coastal plain were probably highs. These highs were in positions that are now occupied by Laramide structures of much greater magnitude. Eolian sandstone deposition occurred downwind (northward) of the Late Jurassic highs. With increasing distance from the source areas, sand supply decreased, causing the northerly thinning of the units.

The localization of Wyoming foreland structures

Structures have developed in roughly the same positions in Wyoming during several episodes of Phanerozoic tectonism. The Laramide mountain ranges and basins are the most recent structures to occupy these positions. The preceding discussion of certain sedimentary facies distributions in the Sundance and Morrison formations demonstrates that structures developed in these positions in the Late Jurassic. From a study of the Phosphoria Formation and its correlatives, Peterson (1980, p. 4) concludes that "sediment thickness and facies patterns suggest the presence of [Permian] paleostructural elements, several of which coincide closely with uplifts and basins of Laramide age."

Tonnsen (1986) using the findings of Sloss (1963) and Vail et al. (1977) notes that the orogenic episodes during which these structures were active correspond to the times of maximum transgression of the North American continent. The major Jurassic and Cretaceous epicontinental seaways existed during one of these major transgressive events (the Zuni sequence of Sloss, 1963). Using terms such as "Wyoming shelf" to describe portions of these tectonically active seaways should be discouraged. This usage connotes a tectonic stability akin to that of continental shelves developed on passive continental margins. Such tectonic stability was not characteristic of the late Mesozoic western interior of North America.

CHAPTER V. CONCLUSION

Stratigraphic Scope of this Study

The sedimentological interpretations presented in this dissertation arose from a study of the uppermost litho-stratigraphic units of the (Upper Jurassic) Sundance Formation. These units, called the coquina facies and sandstone facies in this report, comprise the upper sandstone member of the "upper" Sundance Formation, as described by Imlay (1956). The deposition of these units occurred during the middle to late Oxfordian stage. The terrestrial deposits of the Morrison Formation conformably overlie, and at some localities interfinger with, the uppermost Sundance Formation.

Paleogeographic and Paleoenvironmental Interpretations

General paleogeography

In north-central Wyoming, the uppermost Sundance Formation was deposited along the regressive shoreline of an epicontinental seaway. This shoreline trended generally east-west, with the regression (or the progradation of the Morrison Formation coastal plain) proceeding to the north. This coastline had a mesotidal barrier island morphology within most of the study area. The tidal inlet spacing along this barrier coastline was relatively short. Tidal inlet processes dominated the deposition of the sandstone and coquina facies. Where barrier islands were not developed, the shoreline was characterized by sandy tidal flats.

Paleotectonic influences

The Late Jurassic seaway of the western interior of North America occupied a foreland basin. The regional variation in thickness of the Jurassic strata of the western interior implies that an active orogenic belt existed immediately adjacent to the western margin of the depositional basin. During the Late Jurassic, the frontal thrusts of the Cordilleran orogen occupied a generally north-trending belt from western Utah to eastern British Columbia. East of the orogenic belt, the North American craton subsided in response to the tectonic load. This subsidence, in conjunction with rising global sea level, caused the development of the Late Jurassic seaway.

The regression which controlled the deposition of the uppermost Sundance Formation was driven mainly by tectonic events within the western interior. Eustatic processes did not contribute to this regression, and may have acted to slow the withdrawal of the Oxfordian seaway. Global sea level rose throughout Oxfordian time. Sedimentary infilling of the Late Jurassic foreland basin counteracted the eustatic rise, effectuating the regression.

The areal distribution of dark chert clasts in the uppermost Sundance Formation implies that antiform islands existed within the Oxfordian seaway. These islands were located in the area of the Bighorn Mountains, a principally Laramide-age range. The chert clasts were probably derived from the subaerial erosion of chert-bearing upper Paleozoic units exposed on these islands. The areally coincident, but temporally later development of the Bighorn Mountains has obliterated the most proximal evidence of the Late Jurassic structures.

Depositional setting of the tidal bundle sequences

The tidal bundles within the sandstone facies of the uppermost Sundance Formation were deposited within an environment dominated by asymmetric tidal currents. The large scale trough cross-lamination of the tidal bundles was developed as sinuous-crested megaripples migrated in response to the dominant tidal currents. These megaripples may have been developed on tidal deltas associated with the tidal inlet channels, or on back-barrier shoals. The subordinate tidal currents modified the crests of the megaripples, resulting in the development of sigmoidal reactivation surfaces that truncate the trough cross-lamination sets.

Current ripples migrated across the sigmoidal reactivation surfaces during their development. These current ripples are overlain by mud drapes. The mud drapes represent the sediment deposited from suspension during the times of still water at high and/or low tide. Together, the sigmoidal reactivation surfaces, subordinate current ripples and mud drapes form the set boundaries of the tidal bundles. Cyclic variations in the thickness of the sets of trough cross-lamination in between these bundle boundaries have periods of 9 to 13 bundles per cycle. This periodicity implies that the tidal bundles were most likely developed in a setting characterized by diurnal tides. Sediment transport rate calculations imply that the tidal range along the Late Jurassic coast was at least mesotidal.

REFERENCES

Allen, J.R.L. 1963. The classification of cross-stratified units, with notes on their origin. Sedimentology 2:93-114.

Allen, J.R.L. 1965. Sedimentation in the lee of small underwater sand waves: an experimental study. J. Geol. 73:95-116.

Allen, J.R.L. 1980a. Sand waves: a model of origin and internal structure. Sed. Geol. 26:281-328.

Allen, J.R.L. 1980b. Sand-wave immobility and the internal master bedding of sand-wave deposits. Geol. Mag. 117:437-446.

Allen, J.R.L. 1981a. Lower Cretaceous tides revealed by cross-bedding with mud drapes. Nature 289:579-581.

Allen, J.R.L. 1981b. Paleotidal speeds and ranges estimated from cross-bedded sets with mud drapes. Nature 293:394-396.

Allen, J.R.L. and Friend, P. F. 1976a. Relaxation times of dunes in decelerating aqueous flows. J. Geol. Soc. Lond. 132:17-26.

Allen, J.R.L. and Friend, P. F. 1976b. Changes in intertidal dunes during two spring-neap cycles, Lifeboat Station Bank, Wells-next-the-Sea, Norfolk (England). Sedimentology 23:329-346.

Allen, J.R.L. and Narayan, J. 1964. Cross-stratified units, some with silt bands, in the Folkestone beds (Lower Greensand) of southeast England. Geol. Mijnbw. 43:451-461.

Allen, P. A. and Homewood, P. 1984. Evolution and mechanics of a Miocene tidal sandwave. Sedimentology 31:63-81.

Allmendinger, R. W. and Jordan, T. E. 1981. Mesozoic evolution, hinterland of the Sevier orogenic belt. Geology 9:308-313.

Allmendinger, R. W., Miller, D. M. and Jordan, T. E. 1984. Known and inferred Mesozoic deformation in the hinterland of the Sevier belt, northwest Utah. Utah Geol. Assoc. Publication 14:21-34.

Armstrong, F. C. and Oriel, S. S. 1986. Tectonic development of Idaho-Wyoming thrust belt. pp. 243-280. In J. A. Peterson (ed.). Paleotectonics and sedimentation in the Rocky Mountain region, United States. Memoir 41. Am. Assoc. Petrol. Geol., Tulsa.

Barwis, J. H. and Makurath, J. K. 1978. Recognition of ancient tidal inlet sequences: An example from the Upper Silurian Keyser Limestone in Virginia. Sedimentology 25:61-82.

Beaumont, C. 1981. Foreland basins. Geophys. J. R. Astr. Soc. 65:291-329.

Belderson, R. H. and Stride, A. H. 1966. Tidal current fashioning of a basal bed. Mar. Geol. 4:237-257.

Berg, J. H. van den. 1982. Migration of large-scale bedforms and preservation of crossbedded sets in highly accretional parts of tidal channels in the Oosterschelde, SW Netherlands. Geol. Mijnbw. 61:253-263.

Boersma, J. R. 1967. Remarkable types of mega cross-stratification in the fluviatile sequence of a sub-recent distributary of the Rhine. Geol. Mijnbw. 46:217-235.

Boersma, J. R. 1969. Internal structure of some tidal mega-ripples on a shoal in the Westerschelde Estuary, The Netherlands: Report of a preliminary investigation. Geol. Mijnbw. 48:409-414.

Boersma, J. R., Meene, E. A. van de and Tjalsma, R. C. 1968. Intricated cross-stratification due to interaction of a mega ripple with its lee-side system of backflow ripples (upper-pointbar deposits, Lower Rhine). Sedimentology 11:147-162.

Boersma, J. R. and Terwindt, J.H.J. 1981a. Neap-spring tide sequences of intertidal shoal deposits in a mesotidal estuary. Sedimentology 28:151-170.

Boersma, J. R. and Terwindt, J.H.J. 1981b. Berms on an intertidal shoal: Shape and internal structure. pp. 39-49. In S.-D. Nio, R.T.E. Shuttenhelm and Tj.C.E. van Weering (eds.). Holocene marine sedimentation in the North Sea Basin. Spec. Publ. Int. Assoc. Sediment. Vol. 5. Blackwell Scientific Publications, Oxford.

Brenner, R. L. 1983. Late Jurassic tectonic setting and paleogeography of western interior, North America. pp. 119-132. In M. W. Reynolds and E. D. Dolly (eds.). Mesozoic paleogeography of west-central United States. Rocky Mountain Section, Soc. Econ. Paleont. Miner., Denver.

Brenner, R. L. and Davies, D. K. 1973. Storm-generated coquinoid sandstone: Genesis of high-energy marine sediments from the Upper Jurassic of Wyoming and Montana. Bull. Geol. Soc. Am. 84:1685-1698.

Brenner, R. L. and Davies, D. K. 1974. Oxfordian sedimentation in western interior United States. Bull. Am. Assoc. Petrol. Geol. 58:407-428.

Brenner, R. L., Swift, D.J.P. and Gaynor, G. C. 1985. Re-evaluation of coquinoid sandstone depositional model, Upper Jurassic of central Wyoming and south-central Montana. Sedimentology 32:363-372.

Cobban, W. A. 1945. Marine Jurassic formations of Sweetgrass Arch, Montana. Bull. Am. Assoc. Petrol. Geol. 29:1262-1303.

Crickmay, C. H. 1936. Study in the Jurassic of Wyoming. Bull. Geol. Soc. Am. 47:541-564.

Dalrymple, R. W., Knight, R. J. and Lambiase, J. J. 1978. Bedforms and their hydraulic stability relationships in a tidal environment, Bay of Fundy, Canada. Nature 275:100-104.

Darton, N. H. 1904. Comparison of the stratigraphy of the Black Hills, Bighorn Mountains and Rocky Mountain Front Range. Bull. Geol. Soc. Am. 15:379-448.

Davies, D. K., Ethridge, F. G. and Berg, R. R. 1971. Recognition of barrier environments. Bull. Am. Assoc. Petrol. Geol. 55:550-565.

Dickinson, W. R. 1976. Sedimentary basins developed during evolution of Mesozoic-Cenozoic arc-trench system in western North America. Can. J. Earth Sci. 13:1268-1287.

Dickinson, W. R. 1981. Plate tectonics and the continental margin of California. pp. 1-28. In W. G. Ernst (ed.). The geotectonic development of California. Rubey Vol. 1. Prentice-Hall, New York.

Douglass, D. N. 1984. Stratigraphy and paleomagnetics of the Morrison and Cloverly formations, Bighorn Basin, Wyoming. M. A. Thesis. Dartmouth College, Hanover, New Hampshire.

Elliott, T. 1984. Evidence for diurnal tides in the Upper Jurassic of the western interior basin, U.S.A. p. 34. In Program abstracts, res. symp. sedimentology of shelf sands and sandstones. Can. Soc. Petrol. Geol., Calgary.

Elliott, T. and Gardiner, A. R. 1981. Ripple, megaripple and sandwave bedforms in the macrotidal Loughor Estuary, South Wales, U.K. pp. 51-64 In S.-D. Nio, R.T.E. Shuttenhelm and Tj.C.E. van Weering (eds.). Holocene marine sedimentation in the North Sea Basin. Spec. Publ. Int. Assoc. Sediment. Vol. 5. Blackwell Scientific Publications, Oxford.

Folk, R. L. 1959. The practical petrographical classification of limestones. Bull. Am. Assoc. Petrol. Geol. 43:1-38.

Frey, R. W. and Howard, J. D. 1986. Mesotidal estuarine sequences: A perspective from the Georgia Bight. J. Sed. Petrol. 56:911-924.

Greer, S. A. 1975. Sandbody geometry and sedimentary facies at the estuary-marine transition zone, Ossabaw Sound, Georgia: A stratigraphic model. Senckenberg. Mar. 7:105-135.

Guy, H. R., Simons, D. B. and Richardson, E. V. 1966. Summary of alluvial channel data from flume experiments: 1956-1961. U. S. Geol. Surv. Professional Paper 462-I.

Hayes, M. O. 1975. Morphology of sand accumulations in estuaries: An introduction to the symposium. pp. 3-22. In L. E. Cronin (ed.). Estuarine research, geology and engineering. Vol. 2. Academic Press, London.

Heller, P. L., Bowdler, S. S., Chambers, H. P., Coogan, J. C., Hagen, E. S., Shuster, M. W., Winslow, N. S. and Lawton, T. F. 1986. Time of initial thrusting in the Sevier orogenic belt, Idaho-Wyoming and Utah. Geology 14:388-391.

Homewood, P. and Allen, P. 1981. Wave-, tide-, and current-controlled sandbodies of Miocene Molasse, western Switzerland. Bull. Am. Assoc. Petrol. Geol. 65:2534-2545.

Hoyt, J. H. and Henry, V. J. 1965. Significance of inlet sedimentation in the recognition of ancient barrier islands. pp. 190-194. 19th annual field conference guidebook., Wyoming Geol. Assoc., Casper.

Hoyt, J. H. and Henry, V. J. 1967. Influence of island migration on barrier island sedimentation. Bull. Geol. Soc. Am. 78:77-86.

Hubbard. D. K., Oertal, G. and Nummendal, D. 1979. The role of waves and tidal currents in the development of tidal-inlet sedimentary structures and sand body geometry: Examples from North Carolina, South Carolina and Georgia. J. Sed. Petrol. 49:1073-1092.

Imlay, R. W. 1947. Marine Jurassic of the Black Hills area, South Dakota and Wyoming. Bull. Am. Assoc. Petrol. Geol. 31:227-273.

Imlay, R. W. 1952. Correlation of the Jurassic formations of North America, exclusive of Canada. Bull. Geol. Soc. Am. 63:953-992.

Imlay, R. W. 1956. Marine Jurassic exposed in Bighorn Basin, Pryor Mountains and northern Bighorn Mountains, Wyoming and Montana. Bull. Am. Assoc. Petrol. Geol. 40:562-599.

Imlay, R. W. 1980. Jurassic paleobiogeography of the conterminous United States in its continental setting. U. S. Geol. Surv. Professional Paper 1062.

Kenyon, N. H., Belderson, R. H., Stride, A. H. and Johnson, M. A. 1981. Offshore tidal sand-banks as indicators of net sand transport and as potential deposits. pp. 257-268. In S.-D. Nio, R.T.E. Shuttenhelm and Tj.C.E. van Weering (eds.). Holocene marine sedimentation in the North Sea Basin. Spec. Publ. Int. Assoc. Sediment. Vol. 5. Blackwell Scientific Publications, Oxford.

Klein, G. V. de vries. 1963. Bay of Fundy intertidal zone sediments. J. Sed. Petrol. 33:844-854.

Knight, W. C. 1900. Jurassic rocks of southeastern Wyoming. Bull. Geol. Soc. Am. 11:377-388.

Kreisa, R. D. and Moiola, R. J. 1984. Sigmoidal bundles and other tidal features, Curtis Formation (Jurassic) Utah. Bull. Am. Assoc. Petrol. Geol. 68:497. (abstract)

Kreisa, R. D. and Moiola, R. J. 1986. Sigmoidal tidal bundles and other tide-generated sedimentary structures of the Curtis Formation, Utah. Bull. Geol. Soc. Am. 97:381-387.

Kumar, N. and Sanders, J. E. 1974. Inlet sequence: A vertical succession of sedimentary structures and textures created by the lateral migration of tidal inlets. Sedimentology 21:491-532.

Kvale, E. P. and Vondra, C. F. 1985. Upper Jurassic-Lower Cretaceous transitional marine and fluvial sediments in the Bighorn Basin. pp. 33-44. In R. M. Flores and M. Harvey (eds.). Field guidebook to modern and ancient fluvial systems in the United States. Proc. 3rd Int. Fluvial Sedimentology Conf.

Langhorne, D. N. 1973. A sandwave field in the Outer Thames Estuary, Great Britain. Mar. Geol. 14:129-143.

Love, J. D. 1958. Stratigraphy and fossils of marine Jurassic rocks along the southern margin of the Powder River Basin. pp. 64-70. 13th annual field conference guidebook, Wyoming Geol. Assoc., Casper.

McBride, E. F. 1963. A classification of common sandstones. J. Sed. Petrol. 33:664-669.

McCave, L. N. 1971. Sand waves in the North Sea off the coast of Holland. Mar. Geol. 10:199-225.

Mirsky, A. 1962. Stratigraphy of non-marine Upper Jurassic and Lower Cretaceous rocks, southern Bighorn Mountains, Wyoming. Bull. Am. Assoc. Petrol. Geol. 46:1653-1680.

Moritz, C. A. 1951. Triassic and Jurassic stratigraphy of southwestern Montana. Bull. Am. Assoc. Petrol. Geol. 35:1781-1814.

Mowbray, T. de and Visser, M. J. 1984. Reactivation surfaces in subtidal channel deposits, Oosterschelde, southwest Netherlands. J. Sed. Petrol. 54:811-824.

Narayan, J. 1971. Sedimentary structures in the Lower Greensand of the Weald, England and Bas-Boulonnais, France. Sed. Geol. 6:73-109.

Neely, J. 1937. Stratigraphy of the Sundance Formation and related Jurassic rocks in Wyoming and their petroleum aspects. Bull. Am. Assoc. Petrol. Geol. 21:715-770.

Nio, S. -D. 1976. Marine transgressions as a factor in the formation of sandwave complexes. Geol. Mijnbw. 55:18-40.

Nio, S. -D., Berg, J. H. van den, Goesten, M. and Smulders, F. 1980. Dynamics and sequential analysis of a mesotidal shoal and intershoal channel complex in the Eastern Scheldt (southwestern Netherlands). Sed. Geol. 26:263-279.

Nio, S. -D., Siegenthaler, C. and Yang, C. -S. 1983. Megaripple cross-bedding as a tool for the reconstruction of the palaeo-hydraulics in a Holocene subtidal environment, SW Netherlands. Geol. Mijnbw. 62:499-510.

Odin, G. S. and Matter, A. 1981. De glauconiarum origine. Sedimentology 28:611-641.

Off, T. 1963. Rhythmic linear sand bodies caused by tidal currents. Bull. Am. Assoc. Petrol. Geol. 47:324-341.

Peterson, J. A. 1954. Marine Upper Jurassic, eastern Wyoming. Bull. Am. Assoc. Petrol. Geol. 38:463-507.

Peterson, J. A. 1972. Jurassic System. pp. 177-189. In Geological atlas of the Rocky Mountains. Rocky Mtn. Assoc. Geol., Denver.

Peterson, J. A. 1980. Depositional history and petroleum geology of the Permian Phosphoria, Park City, and Shedhorn formations, Wyoming. U. S. Geol. Surv. Open File Report 80-667:1-42.

Peterson, J. A. and Smith, D. L. 1986. Rocky Mountain paleogeography through geologic time. pp. 3-20. In J. A. Peterson (ed.). Paleotectonics and sedimentation in the Rocky Mountain region, United States. Memoir 31. Am. Assoc. Petrol. Geol., Tulsa.

Pipiringos, G. N. 1968. Correlation and nomenclature of some Triassic and Jurassic rocks in south-central Wyoming. U.S. Geol. Surv. Professional Paper 594-D.

Pipiringos, G. N. and O'Sullivan, R. B. 1978. Principal unconformities in Triassic and Jurassic rocks, western interior United States - a preliminary survey. U. S. Geol. Surv. Professional Paper 1035-A.

Poulton, T. P. 1984. The Jurassic of the Canadian western interior, from 48°N latitude to Beaufort Sea. pp. 15-41. In D. F. Stott and D. J. Glass (eds.). The Mesozoic of middle North America. Memoir 9. Can. Soc. Petrol. Geol., Calgary.

Price, W. A. 1963. Patterns of flow and channeling in tidal inlets. J. Sed. Petrol. 33:279-290.

Raaf, J.F.M. de and Boersma, J. R. 1971. Tidal deposits and their sedimentary structures. Geol. Mijnbw. 50:479-504.

Rautman, C. A. 1978. Sedimentology of Late Jurassic barrier-island complex - Lower Sundance Formation of Black Hills. Bull. Am. Assoc. Petrol. Geol. 62:2275-2289.

Reineck, H. E. 1967. Layered sediments of tidal flats, beaches, and shelf bottom, of the North Sea. pp. 191-206. In G. H. Lauff (ed.). Estuaries. Am. Assoc. Adv. Sci., Washington, D.C.

Reineck, H. E. and Wunderlich, F. 1968. Classification and origin of flaser and lenticular bedding. Sedimentology 11:99-104.

Renfro, H. B. and Feray, D. E. 1972. Geological highway map, northern Rocky Mountain region. Am. Assoc. Petrol. Geol., Tulsa.

Siegenthaler, C. 1982. Tidal cross-strata and the sediment transport rate problem: A geologist's approach. Mar. Geol. 45:227-240.

Sloss, L. L. 1963. Sequences in the cratonic interior of North America. Bull. Geol. Soc. Am. 74:93-114.

Stone, R. and Vondra, C. F. 1972. Sediment dispersal patterns of oolitic calcarenite in the Sundance Formation (Jurassic), Wyoming. J. Sed. Petrol. 42:227-229.

Straaten, L.M.J.U. van. 1950. Environment of formation and facies of the Wadden Sea sediments. Tijdschr. Koninkl. Nederl. Aardv. Genootschap. 67:94-108.

Straaten, L.M.J.U. van. 1954. Composition and structure of recent marine sediments in the Netherlands. Leidse Geol. Med. 19:1-110.

Swain, F. M. and Peterson, J. A. 1951. Ostracoda from the Redwater Shale Member of the Sundance Formation at the type locality in South Dakota. J. Paleont. 25:796-807.

Swift, D.J.P. 1975. Tidal sand ridges and shoal retreat massifs. Mar. Geol. 18:105-134.

Swift, D.J.P., Stanley, D. J. and Curray, J. R. 1971. Relict sediments on continental shelves: a reconsideration. J. Geol. 79:322-346.

Szigeti, G. J. and Fox, J. E. 1981. Unkpapa Sandstone (Jurassic) Black Hills, South Dakota: An eolian facies of the Morrison Formation. pp. 331-349. In F. G. Ethridge and R. M. Flores (eds.). Recent and ancient nonmarine depositional environments: Models for exploration. Special Publ. 31. Soc. Econ. Paleont. Miner., Tulsa.

Terwindt, J.H.J. 1981. Origin and sequences of sedimentary structures in inshore mesotidal deposits of the North Sea. pp. 4-26. In S. -D. Nio, R.T.E. Shuttenhelm and Tj.C.E. van Weering (eds.). Holocene marine sedimentation in the North Sea Basin. Spec. Publ. Int. Assoc. Sediment. Vol. 5. Blackwell Scientific Publications, Oxford.

Terwindt, J.H.J. and Brouwer, M.J.N. 1986. The behaviour of intertidal sandwaves during neap-spring tide cycles and the relevance for palaeoflow reconstructions. Sedimentology 33:1-32.

Teyssen, T.A.L. 1984. Sedimentology of the Minette oolitic ironstones of Luxembourg and Lorraine: A Jurassic subtidal sandwave complex. Sedimentology 31:195-211.

Tonnsen, J. J. 1986. Influence of tectonic terranes adjacent to the Precambrian Wyoming province on Phanerozoic stratigraphy in the Rocky Mountain region. pp. 21-40. In J. A. Peterson (ed.). Paleotectonics and sedimentation in the Rocky Mountain region, United States. Memoir 41. Am. Assoc. Petrol. Geol., Tulsa.

Uhlir, D. M. 1986. Eolian sandstone of Morrison Formation, central Wyoming. Bull. Am. Assoc. Petrol. Geol. 70:1059. (abstract)

Uhlir, D. M. 1987. Subtle tectonics in the Late Jurassic Wyoming foreland: Distribution of Sundance chert and Morrison eolianites. Geol. Soc. Am. Abstracts with Programs 19:339.

Uhlir, D. M. and Vondra, C. F. 1984. Tidal influence in Late Jurassic shallow sea: Evidence from the Sundance Formation, Wyoming. Geol. Soc. Am. Abstracts with Programs 16:680.

Uhlir, D. M., Vondra, C. F., Akers, A. and Elliott, T. 1986. Mesotidal barrier complex, Sundance Formation, north-central Wyoming. Bull. Am. Ass. Petrol. Geol. 70:1059-1060.

Uhlir, D. M., Akers, A. and Vondra, C. F. submitted. Tidal inlet sequence, Sundance Formation (Upper Jurassic) north-central Wyoming. Sedimentology.

Vail, P. R., Mitchum, R. M., Jr., and Thompson, S., III. 1977. Seismic stratigraphy and global changes in sea level. pp. 83-97. In C. E. Payton (ed.). Seismic stratigraphy - applications to hydrocarbon exploration. Memoir 26. Am. Assoc. Petrol. Geol., Tulsa.

Vail, P. R., Hardenbol, J. and Todd, R. G. 1984. Jurassic unconformities, chronostratigraphy, and sea-level changes from seismic stratigraphy and biostratigraphy. pp. 129-144. In J. S. Schlee (ed.). Interregional unconformities and hydrocarbon accumulation. Memoir 36. Am. Assoc. Petrol. Geol., Tulsa.

Visser, M. J. 1980. Neap-spring cycles reflected in Holocene subtidal large-scale bedform deposits: A preliminary note. Geology 8:543-546.

Weed, D. D. and Vondra, C. F. 1987. Implications of an eolian sandstone unit of the basal Morrison Formation, central Wyoming. Bull. Am. Assoc. Petrol. Geol. 71:.

Wilson, J. B. 1982. Shelly faunas associated with temperate offshore tidal deposits. pp. 126-171. In A. H. Stride (ed.). Offshore tidal sands, processes and deposits. Chapman and Hall, London.

Wiltschko, D. V. and Dorr, J. A., Jr. 1983. Timing of deformation in overthrust belt and foreland of Idaho, Wyoming and Utah. Bull. Am. Assoc. Petrol. Geol. 67:1304-1322.

Yang, C. -S. 1986. On Bagnold's sediment transport equation in tidal marine environments and the practical definition of bedload. Sedimentology. 33:465-486.

Yang, C. -S. and Nio, S. -D. 1985. The estimation of palaeohydrodynamic processes from subtidal deposits using time series analysis methods. Sedimentology 32:41-57.

ACKNOWLEDGEMENTS

This research was supported in part by grants from the Standard Oil Company of California and Marathon Oil Company. Support from the Departments of Earth Sciences, Engineering Science and Mechanics and the Engineering Research Institute of Iowa State University is gratefully acknowledged.

Carl Vondra has contributed greatly to many aspects of this research. His interest, criticism and support throughout the course of the research has been invaluable. I am indebted to him for his help in the field, classroom and laboratory. Arthur Akers' expertise, interest and thoughtful insight has greatly benefitted this research. Trevor Elliott was instrumental in the initial phases of this study. The help and generosity of Ralph Specht is greatly appreciated. The writer cherishes field discussions with Paul Wurster. Many thanks to J. David Love, whose consultation has been enlightening and heartening.

The field work was expedited by the efforts of Kat Fennell. The writer is grateful to Richard Beck, Nazrul Khandaker, Erik Kvale, Karen Noggle and Dan Weed for their comments, friendship and support. Sincere thanks to the residents of northern Wyoming, particularly those of Bighorn County, who provided access to their land and gracious hospitality.

APPENDIX A. LOCATIONS OF STRATIGRAPHIC SECTIONS

The locations of the stratigraphic sections measured during the research for this dissertation are presented in this appendix using the township, range and section system of the United States Public Land Survey. The sections are presented in order, from the northernmost to the southernmost township, and from the westernmost to the easternmost range. Each section name is taken from the name of the United States Geological Survey 7.5' or 15' topographic quadrangle map which includes the corresponding section location. Asterisks (*) following section names denote measured sections that are depicted graphically in APPENDIX B.

	SECTION NAME	Section, Township, Range	
1.	BLUEWATER HATCHERY	NE ¼ S8	T 6S R24E
2.	RED DOME	SW ¼ S19	T 7S R24E
3.	COWLEY *	N ½ S22	T58N R96W
4.	SYKES SPRING *	NW ¼ SE ¼ S2	T57N R95W
5.	NORTH EMBLEM RESERVOIR 1	NE ¼ SW ¼ S35	T55N R95W
6.	NORTH EMBLEM RESERVOIR 2	NE ¼ SE ¼ S34	T55N R95W
7.	NORTH EMBLEM RESERVOIR 3 *	NE ¼ S27	T55N R95W
8.	NORTH EMBLEM RESERVOIR 4	SW ¼ NE ¼ S15	T55N R95W
9.	NORTH EMBLEM RESERVOIR 5	NE ¼ S34	T55N R95W
10.	NORTH EMBLEM RESERVOIR 6	SW ¼ S35	T55N R95W
11.	SPENCE 1	S ½ NE ¼ S6	T54N R94W

12.	SPENCE 2	NW ¼ SW ¼ S32	T55N R94W
13.	SPENCE 3	NW ¼ NE ¼ S6	T54N R94W
14.	SPENCE 4	SW ¼ S31	T55N R94W
15.	SPENCE 5	SW ¼ SE ¼ S36	T55N R95W
16.	SPENCE 6	NE ¼ NW ¼ S1	T54N R95W
17.	SPENCE 7	NW ¼ SE ¼ S17	T54N R94W
18.	SPENCE 8	NW ¼ NE ¼ S22	T55N R94W
19.	SPENCE 9	SW ¼ NW ¼ S23	T55N R94W
20.	SPENCE 10	NE ¼ S29	T54N R94W
21.	SPENCE 11	SE ¼ S31	T55N R94W
22.	SPENCE 12	SE ¼ S23	T54N R94W
23.	ALKALI CREEK 1 *	NW ¼ NE ¼ S8	T54N R93W
24.	ALKALI CREEK 2	NW ¼ S12	T54N R94W
25.	LEAVITT RESERVOIR 1 *	NE ¼ S19	T54N R91W
26.	LEAVITT RESERVOIR 2	SE ¼ S18	T54N R91W
27.	LEAVITT RESERVOIR 3	NE ¼ NW ¼ S28	T54N R91W
28.	LEAVITT RESERVOIR 4	SE ¼ S21	T54N R91W
29.	SHELL 1	NW ¼ S34	T54N R91W
30.	SHELL 2 *	NE ¼ S35	T54N R91W
31.	SHELL 3 *	NE ¼ SE ¼ S27	T53N R91W
32.	BLACK MOUNTAIN	NE ¼ S12	T53N R91W
33.	CODY 1 *	SW ¼ S22	T53N R102W
34.	CODY 2 *	S ½ S7	T53N R102W
35.	CODY 3	NW ¼ S17	T53N R102W

36.	CODY 4	SW ¼ NW ¼ S16	T53N R102W
37.	DEVILS TOOTH	NE ¼ S13	T52N R102W
38.	SHEEP CANYON	NW ¼ S3	T53N R94W
39.	WILD HORSE FLATS	NW ¼ S14	T52N R92W
40.	MANDERSON NE 1 *	NE ¼ S10	T51N R91W
41.	MANDERSON NE 2	NE ¼ S15	T52N R91W
42.	MANDERSON NE 3	NW ¼ S15	T52N R91W
43.	MANDERSON NE 4	NE ¼ SW ¼ S11	T52N R92W
44.	MANDERSON NE 5 *	SW ¼ NE ¼ S14	T52N R92W
45.	MANDERSON NE 6	SE ¼ SW ¼ S11	T52N R92W
46.	MANDERSON NE 7	NW ¼ SE ¼ S11	T52N R92W
47.	WHITE SULPHUR SPRING	NE ¼ SE ¼ S11	T52N R91W
48.	WEINTZ DRAW	NE ¼ S19	T49N R89W
49.	HYATTVILLE *	SW ¼ S16	T49N R89W
50.	WILD HORSE HILL	N ½ S21	T48N R89W
51.	JOE EMGE CREEK *	NW ¼ S2	T45N R88W
52.	THERMOPOLIS 1	NW ¼ NE ¼ S4	T42N R94W
53.	THERMOPOLIS 2 *	NW ¼ S24	T43N R95W
54.	THERMOPOLIS 3	NE ¼ S24	T43N R95W
55.	WEDDING OF THE WATERS	NE ¼ SW ¼ S16	T42N R94W
56.	EMBAR	E ½ S4	T8N R2E
57.	RATTLESNAKE GULCH *	NW ¼ S16	T43N R95W
58.	MAHOGANY BUTTE *	W ½ S25	T43N R88W
59.	CORNELL GULCH	NW ¼ S16	T42N R88W

60.	BARNUM	SW ¼ S25	T43N R84W
61.	ROUGHLOCK HILL	S ½ S10	T40N R83W
62.	THREE BUTTES	NW ¼ S25	T39N R86W
63.	DEADMAN BUTTE	NW ¼ S19	T38N R86W
64.	LANDER	SE ¼ S26	T33N R99W
65.	WEISER PASS	SE ¼ S33	T32N R98W
66.	ALCOVA 1	E ½ S35	T30N R83W
67.	ALCOVA 2	SW ¼ S36	T30N R83W
68.	SEMINOE DAM SW	Center S20	T25N R84W

APPENDIX B. GRAPHIC STRATIGRAPHIC SECTIONS

EXPLANATION OF SYMBOLOGY

Sediment Texture:

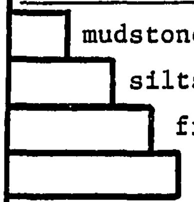

mudstone

siltstone

fine-grained sandstone

medium- and coarse-grained sandstone and coquina

Stratigraphic Thickness:

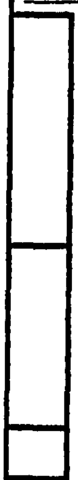

Sedimentary Structures & Paleocurrent Data:

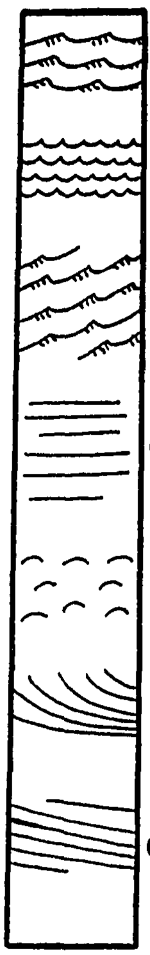

current ripple cross-lamination

000/180 oscillation ripple cross-lamination with north and south oriented paleo-oscillation directions

climbing current ripple cross-lamination

090/270 horizontal lamination with east <u>or</u> west directed paleocurrent direction measured from parting lineation

shells and/or shell fragments

trough cross-lamination

090 epsilon cross-bedding developed by the lateral migration of a channel to the east

COWLEY: N ½ S22 T58N R96W

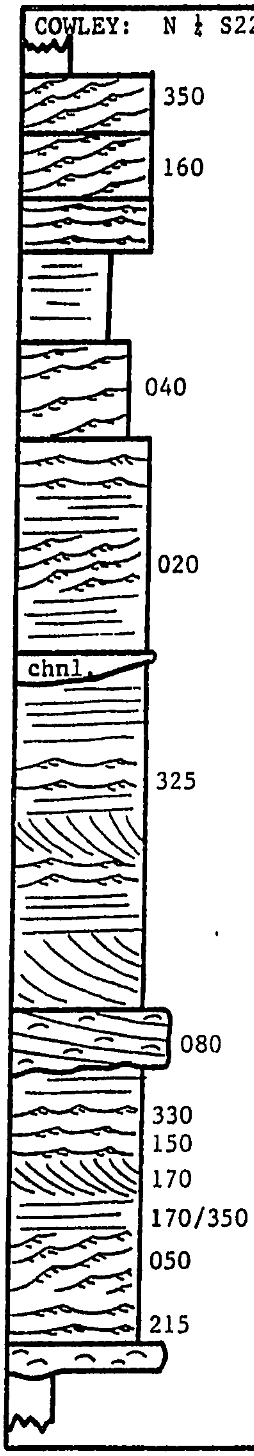

6.1 m MUDSTONE, bentonitic, blue-gray at base, becoming maroon upwards

1.4 m FINE-GRAINED SANDSTONE, no glauconite, climbing current ripple cross-lamination

1.7 m FINE-GRAINED SANDSTONE, glauconitic, climbing current ripple cross-lamination

1.5 m FINE-GRAINED SANDSTONE, no glauconite, current ripple cross-lamination

2.1 m SILTSTONE, green, horizontal lamination

2.2 m VERY FINE-GRAINED SANDSTONE, glauconitic, climbing current ripple cross-lamination with 10° climb angle, 3 cm thick sets

13.5 m FINE-GRAINED SANDSTONE, glauconitic, large-scale (40-70 cm sets) trough cross-lamination, horizontal lamination, current ripple cross-lamination, 1-2 mm mud drapes overlie ripple sets. A 0.7 m deep, 25 m wide channel (chnl.) is incised into horizontally laminated sandstone 8 m up from the base of the unit. The channel is filled with massive, fine-med.-grained glauconitic sandstone, with some finely comminuted shell material with a bright luster. The channel-fill is overlain by horizontally laminated glauconitic fine sandstone, the horizontal lamination grades upwards into climbing ripple cross-lamination

1.4 m FRAGMENTAL COQUINA, fine-grained quartz sand, shell fragment and dark chert (1-2 %) matrix, erosive base (30 cm relief in 2 m) epsilon cross-bedding

6.5 m FINE-GRAINED SANDSTONE, glauconitic, current ripple cross-lamination, horizontal lamination climbing current ripple cross-lamination, 25 cm sets of trough cross-lamination, mud drapes separate stratification sets, region in the vicinity of the drapes is often bioturbated, herringbone current ripple couplets near top of unit

0.7 m FRAGMENTAL COQUINA, abundant belemnites

21.2 m MUDSTONE, lenticular- to flaser-bedded upwrds.

SYKES SPRING: NW ¼ SE ¼ S2 T57N R95W

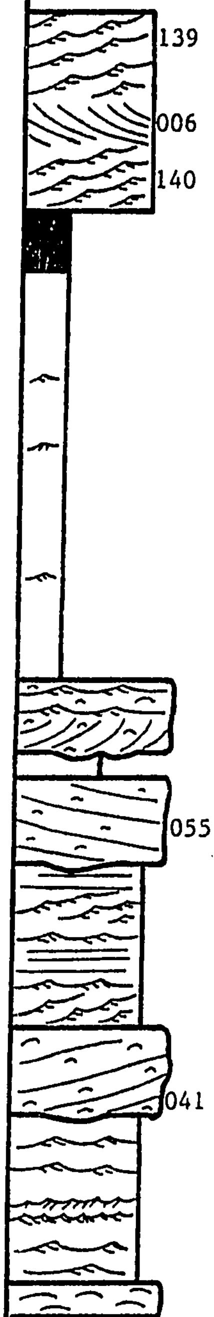

4.5 m FINE-GRAINED SANDSTONE, no glauconite, erosive base (concave-up, 10 cm relief in 1 m) horizontal top of unit, climbing current ripple cross-lam., a 20 cm set of trough cross-lamination

1.5 m MUDSTONE, black, coal fragments, much organic material, spongy when weathered

Morrison Formation

Sundance Formation

9.5 m MUDSTONE, dark blue, occasional 1 cm thick beds of current ripple cross-laminated glauconitic very fine-grained sandstone

1.8 m COQUINOIDAL SANDSTONE, medium-grained, glauc., 10-15 cm sets of trough cross-bedding, current ripple cross-lamination

0.5 m SILTSTONE, dark gray, horizontal lamination

2.0 m COQUINOIDAL SANDSTONE, epsilon cross-bedding fine-grained sandstone

3.9 m FINE-GRAINED SANDSTONE, glauconitic, current ripple cross-lamination, climbing ripple cross-lamination, horizontal lamination

2.2 m FRAGMENTAL COQUINA, 0.5 cm shell fragments in med.-grained sandstone, some dark chert grains, epsilon cross-bedding

4.0 m FINE-GRAINED SANDSTONE, glauconitic, current ripple cross-lamination, some oscillatory current rippleform modification

0.8 m COQUINA, disarticulated, whole Camptonectes tests in silty matrix, 10 cm thick horizontal beds separated by sandy partings

NORTH EMBLEM RESERVOIR 3: NE ¼ S27 T55N R95W

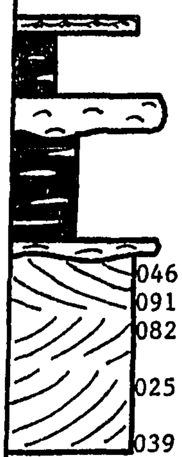

0.2 m FINE-GRAINED SANDSTONE, non-glauconitic, micro-current ripple cross-lamination, bluish white

1.5 m MUDSTONE, mottled red-brown-grey, zones of abundant coal fragments, Fe-oxide staining in assoc. w/coal

0.8 m COQUINA, whole pelecypod tests (0.5 cm diam) in yellow-pink carbonate matrix

2.5 m SILTY MUDSTONE, mottled orange-gray, coal fragments surrounded by yellow gypsiferous crusts

0.4 m COQUINA, concave-down whole *Camptonectes* tests in red-brown quartz sand and shell fragment matrix

4.5 m FINE-GRAINED SANDSTONE, trace glauconite, large-scale trough cross-lamination (eolian?) dark brown spherical concretions (1 cm diam.) in upper part of unit

ALKALI CREEK 1: NW ¼ NE ¼ S8 T54N R93W

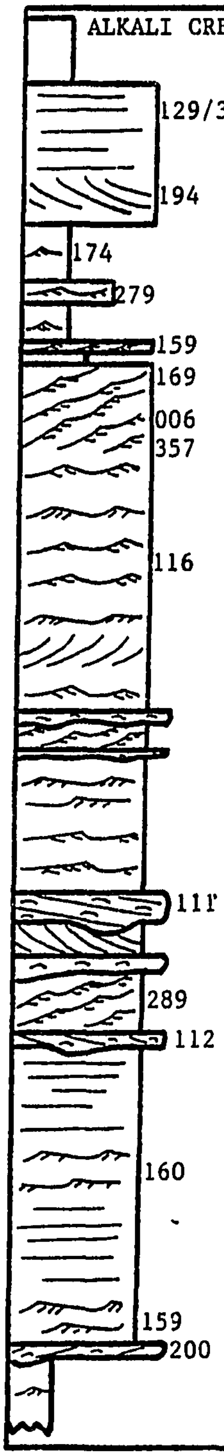

1.3 m MUDSTN., dark gray, Fe-ox. concretions in top 5cm

Morrison Formation

Sundance Formation

3.5 m FINE-GRAINED SANDSTONE, glauconitic, 30 cm sets of trough cross-lamination, horizontal lamination with parting lineation in upper 2 m

1.2 m MUDSTONE, wavy-bedded, with current-rippled siltstone interbeds

0.6 m SILTSTONE, glauc., current ripple cross-lamination

1.0 m MUDSTONE, wavy-bedded, siltstone intercalations

0.2 m FINE-GRAINED SANDSTONE, glauc., climbing ripples

0.2 m SILTY MUDSTONE, horizontal lamination 1 mm thick

8.1 m FINE-GRAINED SANDSTONE, glauconitic, 30 cm sets of trough cross-lamination, lunate current ripples, climbing ripples

0.2 m COQUINA, trough cross-lamination

0.5 m FINE-GRAINED SANDSTONE, glauc., climbing ripples

0.1 m COQUINA

3.1 m FINE-GRAINED SANDSTONE, glauconitic, 2 cm thick sets of current ripple cross-lamination overlain by 1 mm mud drapes

0.8 m FRAGMENTAL COQUINA, epsilon cross-bedding, 1 cm shell fragments in glauconitic sandstone matrix

0.7 m FINE-GRAINED SANDSTONE, glauc., trough cross-lam.

0.4 m FRAGMENTAL COQUINA

1.4 m FINE-GRAINED SANDSTONE, glauc., climbing ripples

0.2 m FRAGMENTAL COQUINA, epsilon cross-bedding

7.0 m FINE-GRAINED SANDSTONE, glauconitic, 5 % dark chert sand grains, current ripple cross-lamination, horizontal lamination

0.3 m FRAGMENTAL COQUINA, medium sandstone matrix, epsilon cross-bedding, % shell frags incr. upwrds

MUDSTONE, dark green-grey, current rippled very fine sandstone interbeds 1-2 cm thick

LEAVITT RESERVOIR 1: NE ¼ S19 T54N R91W

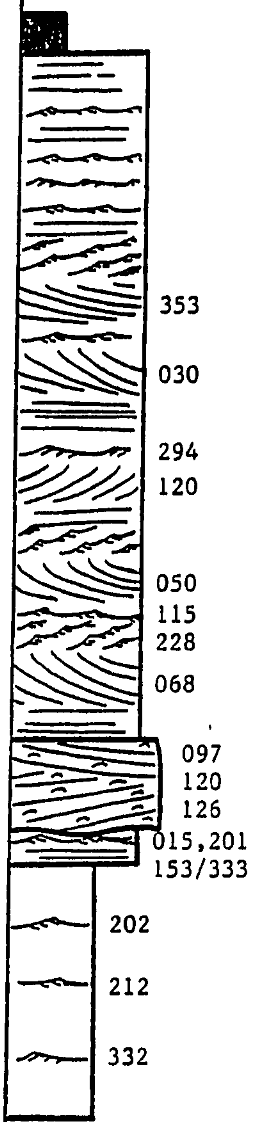

1.1 m MUDSTONE, dark blue-black, occasional lenses of orange mudstn. (surrounding organics?)

Morrison Formation

Sundance Formation

16.5 m FINE-GRAINED SANDSTONE, glauconitic, trough cross-lamination, climbing current ripple cross-lamination, horizontal lamination, 2 mm thick mud drapes overlie the current ripple sets

3.17 m FRAGMENTAL COQUINA, shell fragments, fine-grained sandstone, well-rounded dark chert granules and pebbles, epsilon cross-bedding, erosive base

0.85 m FINE-GRAINED SANDSTONE, glauconitic, 2-4 cm sets of current ripple cross-lamination, 5 cm set of horizontal lamination at base

6.0 m SILTSTONE, with 2-4 cm beds of current ripple cross-laminated very fine-grained sandstone

SHELL 2: NE ¼ S35 T54N R91W

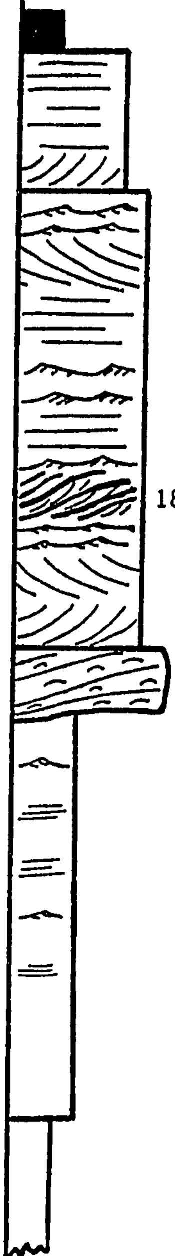

1.1 m MUDSTONE, black, iron-oxide stained nodules in lower 10 cm Of unit

Morrison Formation

Sundance Formation

3.4 m VERY FINE-GRAINED SANDSTONE, glauconitic, percentage of silt increases towards the top of the unit, abundant mud drapes

10.6 m FINE-GRAINED SANDSTONE, glauconitic, large-scale trough cross-lamination, current ripple cross-lamination, horizontal lamination, sets often separated by mud drapes

187 27-bundle tidal bundle sequence

1.5 m FRAGMENTAL COQUINA, shell fragment and quartz sandstone matrix, epsilon cross-bedding

265

9.5 m SILTY MUDSTONE, with thin (1-2 cm) beds of very fine-grained current ripple cross-laminated and horizontal laminated sandstone

40.1 m MUDSTONE, dark gray, abundant large belemnites in slope wash

SHELL 3: NE ¼ SE ¼ S27 T53N R91W

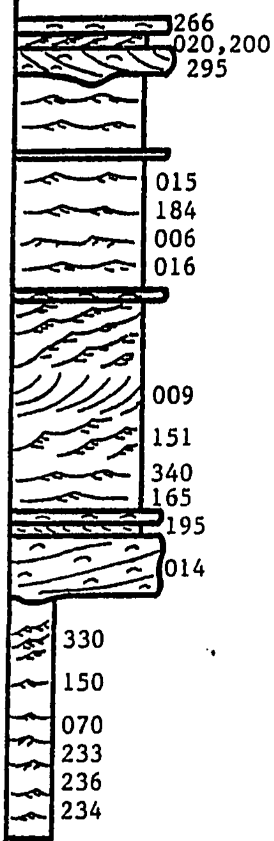

0.3 m	FRAGMENTAL COQUINA, 2-3 cm shell fragments in glauc. fine-med sand matrix, some black chert
0.2 m	FINE-GRAINED SANDSTONE, glauc., climbing ripp.
0.5 m	FRAGMENTAL COQUINA, med. sand and shell frags. single set of trough cross-bedding
1.9 m	FINE-GRAINED SANDSTONE, glauconitic, current ripple cross-lamination, mud drapes
0.1 m	BRECCIA, clast-supported angular fine-grained sandstone fragments in med. glauc. sandstone
3.1 m	FINE-GRAINED SANDSTONE, glauconitic, current ripple cross-lamination, abundant mud drapes
0.2 m	COQUINA, whole Camptonectes in medium-grained sandstone and shell fragment matrix
4.9 m	FINE-GRAINED SANDSTONE, glauconitic, current ripple cross-lamination, climbing current ripple cross-lamination, large scale (50 cm sets) trough cross-lamination
0.1 m	FRAGMENTAL COQUINA, glauc. fine sandstone mtrx
0.1 m	FINE-GRAINED SANDSTONE, mesoripple cross-lam.
1.4 m	FRAGMENTAL COQUINA, epsilon cross-bedding, black chert granules and shell fragments in medium-grained glauconitic sandstone matrix
5.7 m	MUDSTONE, blue-gray, with 2-3 cm thick beds of current ripple cross-laminated very fine-grained sandstone, some oscillation reworking of current ripple sets

CODY 1: SW ¼ S22 T53N R102W

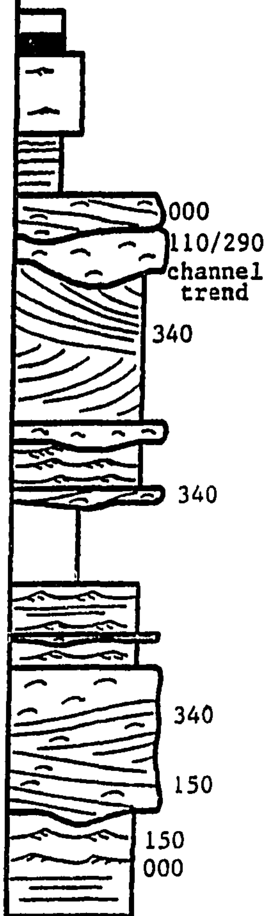

0.4 m	MUDSTONE, bentonitic, light gray
0.3 m	MUDSTONE, coaly, dark grey
	Morrison Formation
	Sundance Formation
2.0 m	SILTY MUDSTONE, olive green, lenticular-bedding, occas. gypsiferous pods around coal clasts
1.5 m	MUDSTONE, 1 mm thick undulatory lamination
0.9 m	COQUINA, silty matrix, shell fragments
1.0 m	COQUINA, whole (Ostrea?) shells in erosive-based channel-fill, channel ca. 1 m deep, 15 m wide
3.4 m	FINE-GRAINED SANDSTONE, glauconitic, 30-50 cm sets of trough cross-lamination
0.4 m	COQUINA, whole, concave-down shells in shell fragment matrix
1.2 m	FINE-GRAINED SANDSTONE, glauc., curr. ripples
0.3 m	COQUINOIDAL SANDSTONE, trough cross-bedding
2.0 m	SILTSTONE, fines upwards to 20 % clay at top, green-brown, fissility increases upwards
1.2 m	FINE-GRAINED SANDSTONE, glauc., current ripp. cross-lam., 1 cm thick horizontal lam. beds
0.2 m	COQUINA, becomes sandier upwards, fragmental
0.5 m	FINE-GRAINED SANDSTONE, glauc., curr. ripples
3.5 m	COQUINOIDAL SANDSTONE, epsilon cross-bedding, 10 cm thick yellow-brown (oxidized?) zone 1.5 m from the base of the unit, coalified wood fragments in the center of the zone
2.6 m	FINE-GRAINED SANDSTONE, glauconitic, horizontal lamination in the lower meter of the unit, herringbone current ripple cross-lamination above, mud drapes overlie ripple sets, scale of ripple sets increases upwards from 0.5 to 2.5 cm near top of unit

CODY 2: S ½ S7 T53N R102W

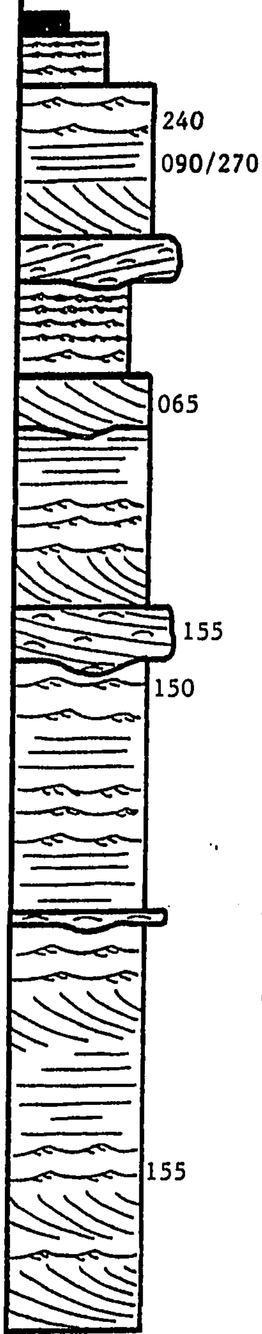

0.5 m MUDSTONE, black, 1 cm coal seams surrounded by crumbly yellow material

Morrison Formation

Sundance Formation

1.2 m VERY FINE-GRAINED SANDSTONE, glauconitic, fining-upwards to brown siltstone, current ripple sets thin upwards from 3 cm to 0.5 cm

3.8 m FINE-GRAINED SANDSTONE, glauconitic, mud drapes separate cross-stratification sets

1.0 m COQUINOIDAL SANDSTONE, shell fragments and fine-grained sandstone

2.7 m VERY FINE-GRAINED SANDSTONE, glauconitic, flaser-bedded 0.5 cm ripple sets near base, cosets thicken upwards, are separated by 0.5 cm dark grey mud drape in upper 20 cm of unit

1.4 m FINE-GRAINED SANDSTONE, less glauconite than underlying and overlying units, large scale trough cross-lamination, erosive base

4.2 m FINE-GRAINED SANDSTONE, 15 % glauconite, dark green, abundant mud rip-up clasts, mud drapes

1.2 m FRAGMENTAL COQUINA, shell fragments in fine-grained quartz sandstone matrix, occasional maroon, tan and black chert granules and well-rounded, sub-spherical pebbles, epsilon cross-bedding

6.0 m FINE-GRAINED SANDSTONE, glauconitic, predominantly horizontally laminated, some current ripple cross-lamination sets overlain by 2 mm mud drapes

0.3 m COQUINA, belemnite tests in shell fragment matrix

9.5 m FINE-GRAINED SANDSTONE, glauconitic, several sequences of trough-current ripple-mud drape repeated from bottom to top of unit, horizontal lamination occasionally overlies current ripple cross-lamination in this sequence, mud drapes are 2 mm thick, dark gray, fissile, bioturbation in upper 15 cm of unit

MANDERSON NE 1: NE ¼ S10 T51N R91W

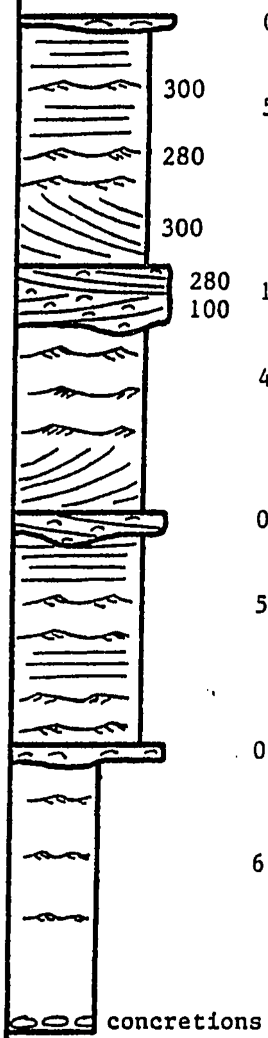

0.2 m COQUINA, 1 cm diam. whole tests in shell fragment matrix, erosive base

5.7 m FINE-GRAINED SANDSTONE, glauconitic, 20-30 cm sets of trough cross-lamination near base of unit, bedform scale descreases upwards, top of unit characterized by 2 cm sets of alternating horizontal lamination and current ripple cross-lamination

1.3 m FRAGMENTAL COQUINA, 20-30 cm sets of trough cross-bedding, erosive base (10 cm in 2 m)

4.4 m FINE-GRAINED SANDSTONE, glauconitic, some silt, large-scale trough cross-lamination in lower 2 m of unit, current ripple cross-lamination above

0.56 m FRAGMENTAL COQUINA, single set of epsilon cross-bedding, erosive base (15 cm in 2 m)

5.1 m FINE-GRAINED SANDSTONE, glauconitic, current ripple cross-lamination, horizontal lamination, sets 0.5-2.0 cm thick

0.15 m COQUINOIDAL SANDSTONE, fine-medium grained sandstone, fine-grained sand to granule-sized shell fragments, erosive base (5 cm in 3 m)

6.4 m SILTSTONE, some clay, 30 cm layer of concretions at base of unit, occasional beds of current ripple cross-laminated very fine-grained sandstone

MANDERSON NE 5: SW ¼ NE ¼ S14 T52N R92W

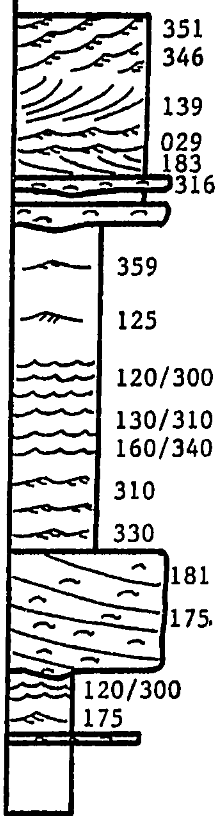

3.7 m FINE- TO VERY FINE-GRAINED SANDSTONE, glauc., some black chert sand grains, abundant mud drapes, macerated organic material and shell fragments in top 50 cm

0.3 m COQUINOIDAL SANDSTONE, trough cross-lamination

0.2 m FINE-GRAINED SANDSTONE, abundant mud drape rip-up clasts

0.4 m FRAGMENTAL COQUINA, % shell fragments decreases upwards, disc-shaped buff siltstone rip-up clasts 1-2 cm diameter

7.7 m SILTSTONE, with 2-3 cm thick beds of current ripple cross-lamination, oscillatory current reworking of some of the current ripple sets

2.8 m FRAGMENTAL COQUINA, epsilon cross-bedding, 2-5 cm shell fragments in glauconitic, fine-grained sandstone matrix, 5 % dark chert sand grains, occasional dark chert granules, silt partings 1 mm thick separate cross-beds

1.4 m SILTY MUDSTONE, lenticular- to wavy-bedded upwards, 1-2 cm thick sets

0.1 m SILTY COQUINA, disarticulated 5 cm whole tests

1.6 m SILTY MUDSTONE, lenticular-bedding

HYATTVILLE: SW ¼ S16 T49N R89W

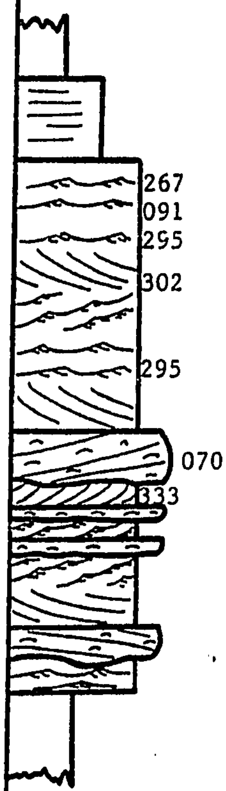

MUDSTONE, variegated, predominantly dark red with dark green and dark grey mottles

Morrison Formation

Sundance Formation

1.75 m SILTSTONE, horizontal lamination, light gray

6.2 m FINE-GRAINED SANDSTONE, glauconitic, large scale trough cross-lamination, lunate current ripples, climbing ripples. Bedform scale decreases upwards

1.1 m FRAGMENTAL COQUINA, epsilon cross-bedding, % shell fragments increases upwards, whole shells in concave-down orientation

0.55 m FINE-GRAINED SANDSTONE, glauconitic, trough cross-lamination

0.25 m COQUINA

0.45 m FINE-GRAINED SANDSTONE, climbing ripple lam.

0.3 m COQUINA, medium sandstone and shell fragments

1.7 m FINE-GRAINED SANDSTONE, glauconitic, sand-sized dark chert grains, trough cross-lam. in 50-90 cm sets, upper 20 cm climbing rippled

0.55 m FRAGMENTAL COQUINA, epsilon cross-bedding

0.85 m FINE-GRAINED SANDSTONE, glauconitic, current ripple cross-lam. in 2 cm sets

SILTY MUDSTONE, pale olive-green, abundant belemnites in slope wash

JOE EMGE CREEK: NW ¼ S2 T45N R88W

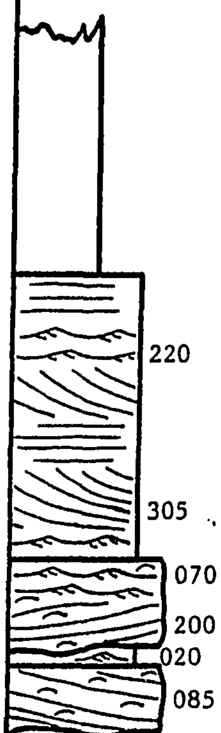

23.4 m SILTY MUDSTONE, fines upwards to mudstone, bentonitic, maroon, light gray mottles

Morrison Formation

Sundance Formation

6.7 m FINE-GRAINED SANDSTONE, glauconitic, large-scale trough cross-lamination, current ripple cross-lamination, horizontal lamination, abundant mud drapes

2.1 m FRAGMENTAL COQUINA, concave-down disarticulated <u>Camptonectes</u> tests in medium sandstone matrix, epsilon cross-bedding, current ripple cross-lamination in upper 30 cm of unit

0.4 m FINE-GRAINED SANDSTONE, glauc., curr. ripples

1.5 m FRAGMENTAL COQUINA, concave-down disarticulated whole tests in fine sand and shell fragment matrix, some dark chert granules and pebbles erosive base (20 cm relief in 1 m, somewhat enhanced by loading into the underlying mudstone

THERMOPOLIS 2: NW ¼ S24 T43N R95W

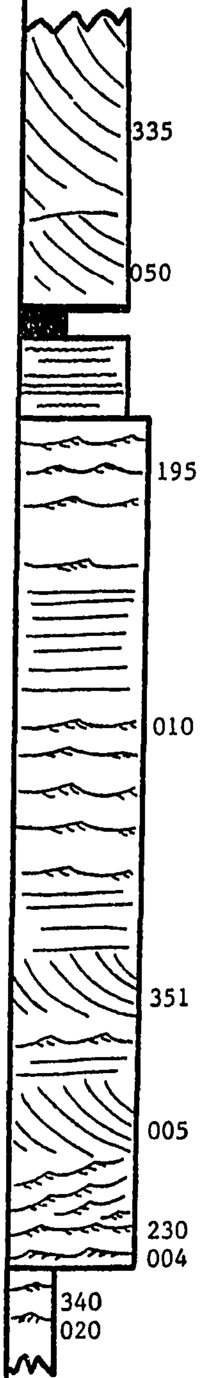

44.7 m VERY FINE-GRAINED SANDSTONE, trace glauconite, very large scale (1-5 m sets) trough cross-lamination (eolian) horizontal, sharp basal contact, unit's top is swaley (dune-form) with a wavelength of approximately 500 m, the unit is overlain by mottled purple-gray-maroon shales

0.7 m MUDSTONE, brown-black, organic material, loading of overlying unit into the upper 10 cm of this unit

Morrison Formation

Sundance Formation

1.9 m VERY FINE-GRAINED SANDSTONE, light gray-white, undulose lamination (adhesion ripples ?) 2 mm wavelength, trace glauconite

19.8 m FINE-GRAINED SANDSTONE, 5 % glauconite, bedform scale increases in lower 6 m, then decreases upwards, slight fining upwards, current ripple cross-lamination and horizontal lamination are the predominant sedimentary structures in the upper half of the unit, mud drapes separate 2 cm oscillation ripple-modified current ripple sets in the upper meter of the unit

MUDSTONE, dark green, with 1-5 cm beds of current ripple cross-laminated very fine-grained glauconitic sandstone

RATTLESNAKE GULCH: NW ¼ S16 T43N R95W

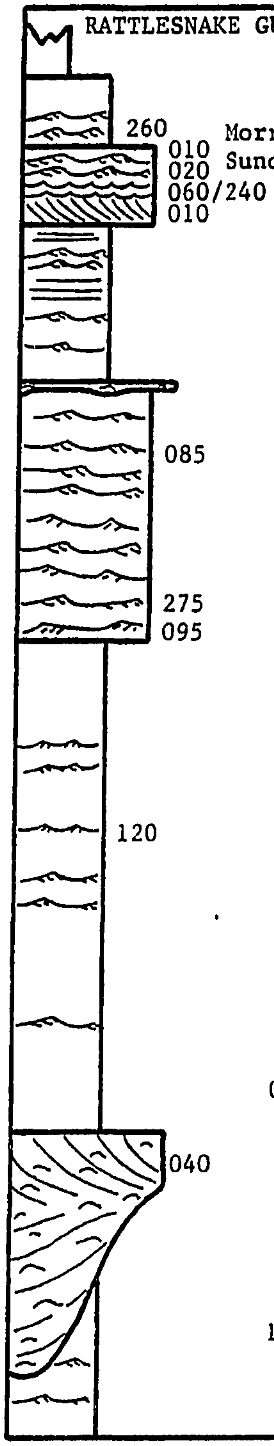

MUDSTONE, mottled maroon and dark gray

1.5 m SILTSTONE, light gray, current ripple lam., unit interfingers w/ eolian sst. to south

Morrison Fm.

Sundance Formation

1.8 m FINE-GRAINED SANDSTONE, glauconitic, skolithos in lower 10 cm of unit

3.9 m MUDSTONE, wavy-bedded, with beds of current ripple cross-laminated and horizontal laminated very fine-grained sandstone, 10 cm thick gypsiferous horizon surrounding organic mattter 2 m above the base of the unit

0.1 m COQUINA, whole shells with pink calcite filling shelter pores under the concave-down shells

5.9 m FINE-GRAINED SANDSTONE, glauconitic, slight coarsening-upwards trend, mud drapes 1 mm thick separate current ripple cross-lamination sets, herringbone current ripple couplets in the lower 40 cm of unit

11.5 m MUDSTONE, wavy-bedded, with beds of current ripple cross-laminated very fine-grained sandstone. Sandstone beds 1-3 cm thick, surrounded by bioturbated mudstone

0-5.8 m COQUINA CHANNEL, 200 m wide, 5.8 m maximum thickness, incised into underlying siltstone, Epsilon cross-beds 1.5-2.0 m thick in center of channel (thickest part of channel). Shell fragments are finely comminuted in central part of channel, shells less fragmented in the thinner, channel margin deposits. 0.8 m thick trough cross-bedding set at top of unit

1.4-7.2 m SILTSTONE, 1-3 cm sets of very fine-grained glauconitic, wavy-flaser-bedded sandstone in horizontally laminated dark grey siltstone

MAHOGANY BUTTE: W ½ S25 T43N R88W

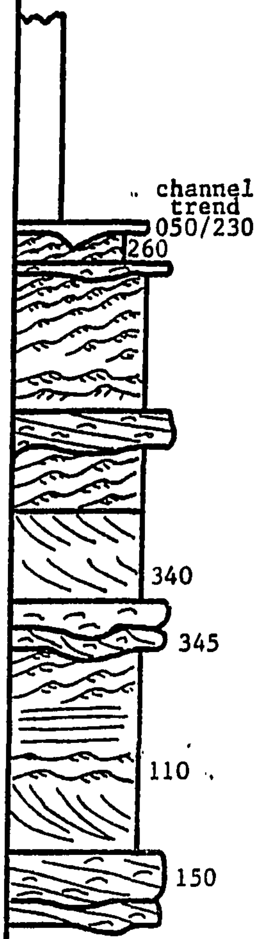

MUDSTONE, bentonitic, mottled gray

0.1-0.5 m FINE-GRAINED SANDSTONE CHANNEL, no glauc., ruddy weathering caste, light gray fresh, massive channel fill

Morrison Formation

Sundance Formation

0.8 m VERY FINE-GRAINED SANDSTONE, glauconitic, climbing ripple cross-lamination

0.3 m COQUINOIDAL SANDSTONE, with angular buff siltstone clasts 1-3 cm in diameter

3.1 m FINE-GRAINED SANDSTONE, glauconitic, climbing current ripple and herringbone current ripple cross-lamination

1.1 m FRAGMENTAL COQUINA, erosive base, faint epsilon cross-bedding, dark chert granules in matrix

1.5 m FINE-GRAINED SANDSTONE, climbing ripple lam.

2.2 m FINE-GRAINED SANDSTONE, glauconitic, large-scale (0.6-0.8 m sets) trough cross-lamination

0.7 m FRAGMENTAL COQUINA, 5 % dark chert clasts

0.5 m COQUINOIDAL SANDSTONE, fine-grained, 25 cm sets of trough cross-bedding

4.7 m FINE-GRAINED SANDSTONE, glauconitic, strat. sequence: trough cross-lam; current ripples; horizontal lamination; climbing current ripples (from bottom to top) rare 1 mm thick mud drapes

1.2 m COQUINA, concave-down whole shells in shell fragment, dark chert and medium-grained quartz sandstone matrix, epsilon cross-bedding

0.6 m COQUINOIDAL SANDSTONE, fine-grained quartz and dark chert sand grains and shell fragments, epsilon cross-bedding

APPENDIX C. QUANTITATIVE ESTIMATE OF PALEOTIDAL RANGE

The tidal bundles of the uppermost Sundance Formation were most likely developed under the influence of asymmetric, diurnal tidal currents. The diurnal nature of these currents is implied from the near 14 bundles per neap-spring cycle. This determination allows an estimate of the rate of megaripple migration to be made. The rate of bedform migration is proportional to the tidal current velocity. The maximum tidal current velocity is especially significant (Allen and Friend, 1976a, 1976b). The maximum tidal current velocity is proportional to the tidal range (Dalrymple et al., 1978). Thus, the paleotidal range of bundle-forming environments may be estimated from the dimensions of the cross-stratification of the bundles. These estimates are made by applying modifications of the formulae of Nio et al. (1983) to the measurements of the tidal bundles at the SHELL 2 locality.

To execute these calculations, several assumptions must be made: (1) the megaripples responsible for the tidal bundles migrated in a regular, linear manner; (2) relatively minor erosion of the megaripple occurred during the subordinate tidal currents; (3) the stratigraphic thickness from the base of the bundle sequences to the organic-rich basal Morrison mudstone is equivalent to the water depth during the bundle development; and (4) approximately 70% of the original megaripple height is preserved in the bundles.

The estimate of original megaripple height, h, is necessary to calculate the bedload transport rate, F, per dominant tide.

$$F_i = hf_i \text{ (effective grain density)/sin BETA}$$

where f_i is the bundle thickness measured in a direction perpendicular to the large scale foresets. The effective grain density includes the effect of buoyancy. The value assumed here is 1650 kg/m^3 and is related through acceleration due to gravity (g = 9.81 m/s^2) to the quantity r_g, which is the buoyancy force per unit grain volume, equal to 1.62(10^4) kg/s^{2}m^2. The value BETA is the inclination of the large scale foresets (23° for the 27-bundle sequence, 25° for the 37-bundle exposure).

The quantity F_i is used in a dimensionless form as:

$$V_i = [2(\text{pi})g(\text{water density})^{1/2}/T(r_g D)^{3/2}]\, F_i$$

where (water density) equals 103 kg/m3 and T is the period of the (diurnal) tidal cycle (8.64 x 10^4 s). The mean grain diameter, D, was determined to be 1.77 x 10^{-4} m.

As there must have been times of slackwater to allow mud drape deposition in between tides, we use time-velocity pattern V from Figure 11 of Nio *et al.* (1983) in which the dimensionless bed transport rate, Z, may be approximated as

$$Z = 3V_i/(pi)$$

The bedload transport rate data of Guy, Simons and Richardson (1966) is used by Nio _et al._ (1983) to construct a portion of their Figure 8. The mean grain diameter of the sandstone facies of the Sundance Formation (1.77×10^{-4} m) is relatively close to the 1.9×10^{-4} m grains used by Guy _et al._ (1966). In order to determine the dimensionless shear velocity, Y, the appropriate experimental points were used for this particular grain size, and it was thus possible to justify values of n = 1 (Figure 8 of Nio _et al._, 1983) and a = 10 (Table I of Nio _et al._, 1983) into:

$$Y_i = (Z/a)^{1/n}$$

to yield the expression:

$$Y_i = Z/10 \text{ , approximately.}$$

The shear velocity (U_*, in m/s) may then be calculated:

$$U_* = (Y_i \, r_g \, D/\text{water density})^{1/2}$$

and finally R, the paleotidal range (in meters) may be estimated:

$$R_i = U_*^2 \, T/(pi)(gH)^{1/2}$$

where H is the water depth, estimated to be 10 m, from the stratigraphic position of the bundles with respect to the basal Morrison mudstone.

The results of these calculations, using the values of 1.0 m and 0.6 m, respectively, for the original heights of the megaripples that developed the 27- and 37-bundle sequences, are summarized below.

Bundle Thickness (m)		Paleotidal Range (m)	
<u>27-Bundle Sequence</u>		(Diurnal)	(Semi-D.)
0.250	mean	3.7	6.3
0.430	maximum spring	6.3	10.8
0.006	minimum neap	0.09	0.15
<u>37-Bundle Sequence</u>			
0.160	mean	1.3	2.2
0.290	maximum spring	2.4	4.0
0.270	mean spring	2.2	3.7
0.008	minimum neap	0.06	0.1
0.033	mean neap	0.3	0.5

(Diurnal) Paleotidal range estimates calculated assuming diurnal tidal periods.

(Semi-D.) Paleotidal range estimates calculated assuming semi-diurnal tidal periods.